

# 15-keto-prostaglandin E<sub>2</sub> activates host peroxisome proliferator-activated receptor gamma (PPAR-γ) to promote *Cryptococcus neoformans* growth during infection.

## Authors:

Robert J. Evans<sup>1,2</sup>, Katherine Pline<sup>1,2</sup>, Catherine A. Loynes<sup>1,2</sup>, Sarah Needs<sup>3</sup>, Maceler Aldrovandi<sup>4</sup>, Jens Tiefenbach<sup>5</sup>, Ewa Bielska<sup>3</sup>, Rachel E. Rubino<sup>6</sup>, Christopher J. Nicol<sup>6</sup>, Robin C. May<sup>3</sup>, Henry M. Krause<sup>5</sup>, Valerie B. O'Donnell<sup>4</sup>, Stephen A. Renshaw<sup>1,2</sup>, Simon A. Johnston<sup>1,2</sup>

<sup>1</sup> Bateson Centre, Firth Court, University of Sheffield, S10 2TN, UK.

<sup>2</sup> Department of Infection, Immunity and Cardiovascular Disease, Medical School, University of Sheffield, S10 2RX, UK.

<sup>3</sup> Institute of Microbiology and Infection, School of Biosciences, University of Birmingham, Birmingham, B15 2TT, UK.

<sup>4</sup> Systems Immunity Research Institute, and Division of Infection and Immunity, School of Medicine, Cardiff University, Cardiff CF14 4XN, UK

<sup>5</sup> Banting and Best Department of Medical Research, The Terrence Donnelly Centre for Cellular and Biomolecular Research (CCBR), University of Toronto, Toronto, Ontario, Canada, InDanio Bioscience Inc., Toronto, Ontario, Canada

<sup>6</sup> Department of Pathology and Molecular Medicine, Queen's University, Kingston, ON, Canada.

Running Title: Fungal derived 15-keto-prostaglandin E<sub>2</sub> and PPAR-γ promote *C. neoformans* infection

\*Author for correspondence: Simon A. Johnston

Email: s.a.johnston@sheffield.ac.uk



## Abstract

*Cryptococcus neoformans* is one of the leading causes of invasive fungal infection in humans worldwide. *C. neoformans* uses macrophages as a proliferative niche to increase infective burden and avoid immune surveillance. However, the specific mechanisms by which *C. neoformans* manipulates host immunity to promote its growth during infection remain ill-defined. Here we demonstrate that eicosanoid lipid mediators manipulated and/or produced by *C. neoformans* play a key role in regulating pathogenesis. *C. neoformans* is known to secrete several eicosanoids that are highly similar to those found in vertebrate hosts. Using eicosanoid deficient cryptococcal mutants  $\Delta plb1$  and  $\Delta lac1$ , we demonstrate that prostaglandin  $E_2$  is required by *C. neoformans* for proliferation within macrophages and *in vivo* during infection. Genetic and pharmacological disruption of host  $PGE_2$  synthesis is not required for promotion of cryptococcal growth by eicosanoid production. We find that  $PGE_2$  must be dehydrogenated into 15-keto- $PGE_2$  to promote fungal growth, a finding that implicated the host nuclear receptor  $PPAR-\gamma$ . *C. neoformans* infection of macrophages activates host  $PPAR-\gamma$  and its inhibition is sufficient to abrogate the effect of 15-keto- $PGE_2$  in promoting fungal growth during infection. Thus, we describe the first mechanism of reliance on pathogen-derived eicosanoids in fungal pathogenesis and the specific role of 15-keto- $PGE_2$  and host  $PPAR-\gamma$  in cryptococcosis.

## Author Summary:

*Cryptococcus neoformans* is an opportunistic fungal pathogen that is responsible for significant numbers of deaths in the immunocompromised population worldwide. Here we address whether eicosanoids produced by *C. neoformans* manipulate host innate immune cells during infection. *Cryptococcus neoformans* produces several eicosanoids that are notable for their similarity to vertebrate eicosanoids, it is therefore possible that fungal-derived eicosanoids may provoke physiological effects in the host. Using a combination of *in vitro* and *in vivo* infection models we identify a specific eicosanoid species - prostaglandin  $E_2$  – that is required by *C. neoformans* for

growth during infection. We subsequently show that prostaglandin  $E_2$  must be converted to 15-keto-prostaglandin  $E_2$  within the host before it has these effects. Furthermore, we find that prostaglandin  $E_2$ /15-keto-prostaglandin  $E_2$  mediated virulence is via activation of host PPAR- $\gamma$  – an intracellular eicosanoid receptor known to interact with 15-keto-PGE $_2$ .

## Introduction

*Cryptococcus neoformans* is an opportunistic pathogen that infects individuals who have severe immunodeficiencies such as late-stage HIV AIDS. *C. neoformans* is estimated to infect 278,000 individuals each year resulting in 181,000 deaths (1,2). *C. neoformans* infection begins in the lungs where the fungus is phagocytosed by host macrophages. Macrophages must become activated by further inflammatory signals from the host immune system before they can effectively kill *C. neoformans* (3,4). When this does not occur *C. neoformans* proliferates rapidly intracellularly and may use the macrophage to disseminate to the central nervous system leading to fatal cryptococcal meningitis (5-9).

Eicosanoids are an important group of lipid inflammatory mediators produced by innate immune cells such as macrophages. Eicosanoids are a diverse group of potent signalling molecules that have a short range of action and signal through autocrine and paracrine routes. Macrophages produce large amounts of a particular group of eicosanoids called prostaglandins during microbial infection (10,11). Prostaglandins have a number of physiological effects throughout the body, but in the context of immunity they are known to strongly influence the inflammatory state (12). The prostaglandins PGE $_2$  and PGD $_2$  are the best-studied eicosanoid inflammatory mediators. During infection, macrophages produce both PGE $_2$  and PGD $_2$  to which, via autocrine routes, they are highly responsive (12). In vertebrate immunity, the synthesis of eicosanoids such as PGE $_2$  is carefully regulated by feedback loops to ensure that the potent effects of these molecules are properly constrained. Exogenous sources of eicosanoids within the body, such as

from eicosanoid-producing parasites (13) or tumours that overproduce eicosanoids (14,15), can disrupt host inflammatory signaling as they are not subject to the same regulation.

It is well known that *C. neoformans* produces its own eicosanoid species. These fungal-derived eicosanoids are indistinguishable from those produced by vertebrates (16-18). Only two *Cryptococcus* enzymes are known to be associated with cryptococcal eicosanoid synthesis - phospholipase B1 and laccase (18,19). Deletion of phospholipase B1 reduces secreted levels of all eicosanoids produced by *C. neoformans* suggesting that it has high level role in eicosanoid synthesis (19), perhaps fulfilling the role of phospholipase A<sub>2</sub> in higher organisms. Deletion of laccase results in reduced levels of PGE<sub>2</sub> but other eicosanoids are unaffected suggesting that laccase has putative PGE<sub>2</sub> synthase activity (18). *C. neoformans* produces eicosanoids during infection, these eicosanoids are indistinguishable from host eicosanoids so it is possible that *C. neoformans* is able to manipulate the host inflammatory state during infection by directly manipulating host eicosanoid signaling.

It has previously been reported that the inhibition of prostaglandin E<sub>2</sub> receptors EP2 and EP4 during murine pulmonary infection leads to better host survival accompanied by a shift towards Th1/M1 macrophage activation, however it was not determined if PGE<sub>2</sub> was derived from the host or the fungus (20). Therefore, a key aspect of *C. neoformans* pathogenesis remains unanswered: do eicosanoids produced by *C. neoformans* manipulate host innate immune cells function during infection?

We have previously shown that the eicosanoid deficient strain  $\Delta plb1$  has reduced proliferation and survival within macrophages (21). We hypothesised that eicosanoids produced by *C. neoformans* support intracellular proliferation within macrophages and subsequently promote pathogenesis. To address this hypothesis, we combined *in vitro* macrophage infection assays

with our previous published *in vivo* zebrafish model of cryptococcosis (22). We found that PGE<sub>2</sub> was sufficient to promote growth of  $\Delta plb1$  and  $\Delta lac1$  independent of host PGE<sub>2</sub> production, *in vitro* and *in vivo*. We show that the effects of PGE<sub>2</sub> in cryptococcal infection are mediated by its dehydrogenated form, 15-keto-PGE<sub>2</sub>. Finally, we determine that 15-keto-PGE<sub>2</sub> promotes *C. neoformans* infection via the activation of the host nuclear transcription factor PPAR- $\gamma$ , demonstrating that 15-keto-PGE<sub>2</sub> and PPAR- $\gamma$  are new factors in cryptococcal infection

## Results

### *Prostaglandin E<sub>2</sub> is required for C. neoformans growth in macrophages*

We have previously shown that the *C. neoformans* mutant strain  $\Delta plb1$  has impaired proliferation and survival within J774 murine macrophages *in vitro* (21). The  $\Delta plb1$  strain has a deletion in the *PLB1* gene which codes for the secreted enzyme phospholipase B1 (23). The  $\Delta plb1$  strain is known to produce lower levels of fungal eicosanoids indicating that phospholipase B1 is involved in fungal eicosanoid synthesis (19). It has been proposed that the attenuation of this strain within macrophages could be because it cannot produce eicosanoids (19). A previous study has identified PGE<sub>2</sub> as an eicosanoid that promotes cryptococcal virulence and manipulates macrophage activation, however this study did not determine if PGE<sub>2</sub> was produced by the host or *C. neoformans* (20). We hypothesised that PGE<sub>2</sub> - or other phospholipase B1 derived eicosanoid species - are produced by *C. neoformans* during infection and promote macrophage infection.

To test if PGE<sub>2</sub> promotes the intracellular growth of *C. neoformans* we treated  $\Delta plb1$  infected J774 macrophages with exogenous PGE<sub>2</sub> and measured intracellular proliferation over 18 hours. The addition of exogenous PGE<sub>2</sub> to J774 macrophages infected with  $\Delta plb1$  was sufficient to recover the intracellular proliferation of  $\Delta plb1$  compared to the H99 (parental wild type strain)

and  $\Delta plb1:PLB1$  (reconstituted strain) strains (Fig 1  $p=0.038$ ). These findings support our initial hypothesis and identify  $PGE_2$  as a mediator of cryptococcal virulence during macrophage infection.

We have previously shown that  $\Delta plb1$  has reduced intracellular proliferation due to a combination of reduced cell division and reduced viability within the phagosome (21). In our intracellular proliferation assay the number of intracellular *Cryptococcus* cells is quantified by lysing infected macrophage and counting the number of *Cryptococcus* cells with a hemocytometer. Due to their structurally stable fungal cell wall dead or dying *Cryptococcus* cells do not look noticeably different on a hemocytometer from viable cells. To quantify the viability of *Cryptococcus* cells retrieved from the phagosome we diluted the lysate to give an expected number of CFUs (in this case 200 CFU), spread the diluted lysate on YPD agar and count the actual number of CFUs produced – a difference between the expected CFU count (200 CFU) and the actual CFU count indicates a loss of *Cryptococcus* cell viability. In this case viability assays showed that exogenous  $PGE_2$  produced no significant increase in the viability of  $\Delta plb1$  cells within the phagosome (Supplementary Fig 1A).

### *Exogenous prostaglandin E<sub>2</sub> rescues in vivo growth of $\Delta plb1$ -GFP*

Our *in vitro* data showed that  $PGE_2$  promotes the intracellular proliferation of *C. neoformans* within macrophages. First, we injected 2-day post fertilisation (dpf) zebrafish larvae with  $\Delta plb1$ -GFP (a constitutively expressed GFP tagged version of the  $\Delta plb1$  generated for this study). One of the advantages of this model is that the fungal burden can be non-invasively imaged within infected larvae using fluorescently tagged *C. neoformans* strains and we able measure the growth of the fungus at 1-, 2- and 3-days post-infection (dpi). We found that  $\Delta plb1$ -GFP infected larvae had significantly lower fungal burdens at 1, 2- and 3-days post infection (Fig 2D and Supplementary Fig 1B) compared to the parental strain H99-GFP (Fig 2A and Supplementary

Fig 1B). These data demonstrated that the  $\Delta plb1$ -GFP mutant had a similar growth deficiency to our *in vitro* phenotype and with previous studies (21,23,24). To confirm that PGE<sub>2</sub> promotes cryptococcal infection *in vivo* we infected zebrafish larvae with  $\Delta plb1$ -GFP or H99-GFP and treated the larvae with exogenous PGE<sub>2</sub>. In agreement with our *in vitro* findings (Fig 1), exogenous PGE<sub>2</sub> increased the growth of both the parental H99 strain (Fig 2B, p = 0.0137, 1.35-fold increase vs. DMSO) and the  $\Delta plb1$ -GFP mutant (Fig 2E, p= 0.0001, 2.15-fold increase vs. DMSO) while PGD<sub>2</sub> did not (Fig 2C and 2F). Taken together these data show that PGE<sub>2</sub> is sufficient to enhance the virulence of *C. neoformans* *in vivo*, furthermore our *in vitro* data suggest that this is a result of uncontrolled intracellular proliferation within macrophages (Fig 1).

*Prostaglandin E<sub>2</sub> must be dehydrogenated into 15-keto-PGE<sub>2</sub> to promote C. neoformans growth.*

PGE<sub>2</sub> can be enzymatically and non-enzymatically modified in cells to form a number of distinct metabolites. To distinguish the biological activity of PGE<sub>2</sub> rather than its metabolites we used an analogue of PGE<sub>2</sub> called 16,16-dimethyl PGE<sub>2</sub> that cannot be dehydrogenated but otherwise has comparable activity to PGE<sub>2</sub> (25)). We found that unlike PGE<sub>2</sub>, 16,16-dimethyl PGE<sub>2</sub> treatment did not increase the fungal burden of  $\Delta plb1$ -GFP (Fig 3C p= 0.9782) or H99-GFP infected larvae (Fig 3A p= 0.9954). Therefore, the biological activity of PGE<sub>2</sub> alone did not appear to promote cryptococcal pathogenesis and that dehydrogenation of PGE<sub>2</sub> was required. PGE<sub>2</sub> and 16,16-dimethyl PGE<sub>2</sub> both signal through PGE<sub>2</sub> receptors (EP1, EP2, EP3 and EP4) but 15-keto-PGE<sub>2</sub> does not. In a murine model of pulmonary cryptococcosis the PGE<sub>2</sub> receptors EP2 and EP4 have been identified as promoters of fungal virulence (20). To confirm that PGE<sub>2</sub> itself does not promote virulence in our model we treated zebrafish with antagonists against the EP2 and EP4 receptors. In support of our previous experiment we found that EP2 / EP4 inhibition had no effect on fungal burden in zebrafish (Fig 3E). An abundant dehydrogenated form of PGE<sub>2</sub> is 15-keto-PGE<sub>2</sub> (that has also been isolated from *C. neoformans* (18)) and we tested if 15-keto-PGE<sub>2</sub>



was sufficient to rescue the growth defect of the  $\Delta plb1$  mutant during infection. Therefore, we treated infected zebrafish larvae with exogenous 15-keto-PGE<sub>2</sub> and found that this was sufficient to significantly increase the fungal burden of zebrafish larvae infected with both  $\Delta plb1$ -GFP (Fig 3D,  $p = 0.0119$ , 1.56-fold increase vs. DMSO) and H99-GFP (Fig 3B,  $p = 0.0048$ , 1.36-fold increase vs. DMSO). To explore the *Cryptococcus* eicosanoid synthesis pathway further we used a second eicosanoid deficient *C. neoformans* mutant  $\Delta lac1$ . Whereas  $\Delta plb1$  is unable to produce any eicosanoid species  $\Delta lac1$  is deficient only in PGE<sub>2</sub> and 15-keto-PGE<sub>2</sub> (18). Using a  $\Delta lac1$ -GFP strain generated for this study we found that  $\Delta lac1$ -GFP also produced low fungal burden during *in vivo* zebrafish larvae infection (Supplementary Fig 2B). As with  $\Delta plb1$ -GFP, this defect could be rescued with the addition of exogenous PGE<sub>2</sub> (Supplementary Fig 2C), but not with 16,16-dm-PGE<sub>2</sub> (Supplementary Fig 2D) or with 15-keto-PGE<sub>2</sub> (Supplementary Fig 2E). Prostaglandin E<sub>2</sub> is known to affect haematopoietic stem cell homeostasis in zebrafish (26). This could affect macrophage number and subsequently fungal burden. We have previously observed that a large depletion of macrophages can lead to increased fungal burden in zebrafish larvae (22). We performed whole body macrophage counts on 2 dpf uninfected larvae treated with PGE<sub>2</sub> or 15-keto-PGE<sub>2</sub> 2 days post treatment (the same time points used in our infection assay). Following PGE<sub>2</sub> and 15-keto PGE<sub>2</sub> treatment macrophages were still observable throughout the larvae. For PGE<sub>2</sub> treatment we saw on average a 15% reduction in macrophage number while 15-keto PGE<sub>2</sub> did not cause any decrease (Supplementary Fig 1C). Due to the fact that fungal burden increased during both PGE<sub>2</sub> and 15-keto PGE<sub>2</sub> treatments it is highly unlikely that this reduction could account for the increases in burden seen.

*Host derived prostaglandins are not required for growth of C. neoformans*

After determining that PGE<sub>2</sub> promotes the growth of *C. neoformans* *in vitro* and *in vivo* via its metabolite 15-keto-PGE<sub>2</sub>, we wanted to determine whether the source of these prostaglandins was the host or the fungus. Our *in vitro* data show that the *C. neoformans* strain  $\Delta plb1$  has a growth deficiency *in vitro* and *in vivo* that can be rescued with the addition of PGE<sub>2</sub>, because this phenotype is mediated by cryptococcal phospholipase B1 it indicates that pathogen-derived rather than host-derived prostaglandins are required. A previous study reports that *C. neoformans* infection can induce higher PGE<sub>2</sub> levels in the lung during *in vivo* pulmonary infection of mice (20), although it was not determined if the PGE<sub>2</sub> was host or pathogen derived. Therefore, we tested the hypothesis that host prostaglandin synthesis was not required for cryptococcal virulence.

To block host prostaglandin synthesis *in vitro* we inhibited host cyclooxygenase activity because it is essential for prostaglandin synthesis in vertebrates (27). We treated H99 and  $\Delta plb1$  infected J774 macrophages with aspirin at a concentration we determined was sufficient to block host PGE<sub>2</sub> synthesis (Supplementary Fig 3A). Aspirin is a non-reversible inhibitor of cyclooxygenase 1 (COX-1) and cyclooxygenase 2 (COX-2) enzymes, we therefore included a condition where J774 cells were pretreated with aspirin only prior to infection and then at a condition where aspirin was present throughout infection. We found that aspirin treatment did not affect the intracellular proliferation of H99 or  $\Delta plb1$  (Fig 4A), suggesting that host cyclooxygenase activity is not required for the phospholipase B1 dependent virulence of *C. neoformans* during macrophage infection. To confirm these *in vivo*, we pharmacologically blocked zebrafish cyclooxygenase-1 (COX-1) and cyclooxygenase-2 (COX-2). We used separate cyclooxygenase inhibitors with zebrafish larvae instead of aspirin because we found that aspirin treatment led to lethal developmental defects in zebrafish larvae (unpublished observation). We infected 2 dpf zebrafish larvae with H99-GFP and  $\Delta plb1$ -GFP and treated with inhibitors for COX-1 (NS-398, 15  $\mu$ M) and COX-2 (SC-560, 15  $\mu$ M). We found that both inhibitors decreased the fungal burden

of H99-GFP, but not  $\Delta plb1$ -GFP infected zebrafish larvae (Fig 4B i and 4B ii, H99-GFP - NS-398,  $p=0.0002$ , 1.85-fold decrease vs. DMSO. SC-560  $p<0.0001$ , 3.14-fold decrease vs DMSO). These findings were different to what we had observed *in vitro* but because this phenotype was phospholipase B1 dependent we reasoned that these inhibitors could be having off target effects on *C. neoformans* - although *C. neoformans* does not have a homolog to cyclooxygenase other studies have tried to inhibit eicosanoid production in *Cryptococcus* using cyclooxygenase inhibitors but their efficacy and target remain uncertain (17,28). To support our pharmacological evidence, we used a CRISPR/Cas9-mediated knockdown of the prostaglandin  $E_2$  synthase gene (*ptges*) (29). We used a knockdown of tyrosinase (*tyr*) – a gene involved in the conversion of tyrosine into melanin as a control because *tyr*<sup>-/-</sup> crispants are easy to identify because they do not produce any pigment. We infected 2 dpf *ptges*<sup>-/-</sup> and *tyr*<sup>-/-</sup> zebrafish larvae with H99-GFP or  $\Delta plb1$ -GFP and measured the fungal burden at 3 dpi. We found that *ptges*<sup>-/-</sup> zebrafish infected with H99-GFP had a higher fungal burden at 3 dpi compared to *tyr*<sup>-/-</sup> zebrafish infected with H99-GFP whereas there was no difference between *ptges*<sup>-/-</sup> and *tyr*<sup>-/-</sup> zebrafish larvae infected with  $\Delta plb1$ -GFP (Fig 4C). Thus, both pharmacological and genetic inhibitions of host prostaglandin synthesis were not determinants of *C. neoformans* growth.

#### Phospholipase B1 dependent factors are sufficient to support $\Delta plb1$ growth in macrophages

To further evidence that *C. neoformans* was the source of PGE<sub>2</sub> during macrophage infection we used a co-infection assay which has previously been used to investigate the interaction of different *C. gattii* strains within the same macrophage (30). We hypothesised that if *C. neoformans* derived prostaglandins promoted fungal growth, co-infection between H99 and  $\Delta plb1$  would support mutant growth within macrophages because the parental strain H99 would produce growth promoting prostaglandins that are lacking in  $\Delta plb1$ . To produce co-infection, J774 murine macrophages were infected with a 50:50 mixture of  $\Delta plb1$  and H99-GFP (31) (Fig

4E i; as described previously for *C. gattii* (30)). This approach allowed us to differentiate between  $\Delta plb1$  (GFP negative) and H99 (GFP positive) *Cryptococcus* strains within the same macrophage and to score their proliferation separately. The intracellular proliferation of  $\Delta plb1$  was calculated by counting the change in number of GFP negative  $\Delta plb1$  cells over an 18hr period from time-lapse movies of infected cells. We found that co-infected macrophages did not always contain an equal ratio of each strain at the start of the 18hr period so we scored the proliferation of  $\Delta plb1$  for a range of initial burdens (1:2, 1:3 and 1:4). We found that  $\Delta plb1$  proliferated better when accompanied by two H99-GFP yeast cells in the same macrophage (Fig 4E ii, 1:2  $p = 0.014$ ) as opposed to when two  $\Delta plb1$  yeast cells were accompanied by one H99-GFP yeast cell (Fig 4E ii, 2:1). We observed a similar effect for ratios of 1:3 and 1:4, but these starting burden ratios are particularly rare, under powering our analysis (Supplementary Fig 3). This effect was also recapitulated for J774 macrophages co-infected with  $\Delta lac1$  and H99-GFP (Supplementary Fig 2A). These data indicate that a phospholipase B1 dependent factor found in H99 infected macrophages, but absent in  $\Delta plb1$  and  $\Delta lac1$  infected macrophages, is required for intracellular proliferation within macrophages.

#### *Production of PGE<sub>2</sub> by macrophages is not altered by C. neoformans infection.*

Our data indicate that host cells are not the source of virulence promoting prostaglandins, and that secreted factors produced by wild type - but not  $\Delta plb1$  or  $\Delta lac1$  *Cryptococcus* strains – promote fungal growth within macrophages. We wanted to test if there were detectable difference in PGE<sub>2</sub> levels between infected and uninfected macrophages caused by cryptococcal prostaglandin synthesis. To do this we performed ELISA analysis to detect PGE<sub>2</sub> concentrations in supernatants from *C. neoformans* infected J774 macrophages (Fig 4D i). We found that J774 macrophages produced detectable levels of PGE<sub>2</sub> (mean concentration 4.10 ng/1x10<sup>6</sup> cells), however we did not see any significant difference between infected or

uninfected macrophages (infected with H99,  $\Delta plb1$  or  $\Delta plb1:PLB1$  strains). To confirm our ELISA results, we performed LC MS/MS analysis of lysed J774 macrophages using a PGE<sub>2</sub> standard for accurate quantification (Fig 4D ii). The concentrations detected were similar to those measured by our ELISA (mean concentration 6.35 ng/1X10<sup>6</sup> cells) and also did not show any significant differences between conditions. Taken together these data suggest that any *Cryptococcus*-derived prostaglandins present during infection were likely to be contained within the macrophage in low, localized concentrations and that the host receptor targeted by these eicosanoids is therefore likely to be intracellular.

#### *15-keto-PGE<sub>2</sub> promotes C. neoformans growth by activating host PPAR- $\gamma$*

We next wanted to determine how PGE<sub>2</sub> / 15-keto-PGE<sub>2</sub> promotes *C. neoformans* infection. We hypothesized that these prostaglandins were interfering with inhibition of fungal growth via a host receptor. Our experiments inhibiting EP2 / EP4 suggest that 15-keto-PGE<sub>2</sub> must signal through a different receptor to PGE<sub>2</sub> (Fig 3E). 15-keto-PGE<sub>2</sub> is a known agonist of the peroxisome proliferation associated receptor gamma (PPAR- $\gamma$ ) (32); a transcription factor that controls expression of many inflammation related genes (33-35). We first tested if PPAR- $\gamma$  activation occurs within macrophages during *C. neoformans* infection by performing immunofluorescent staining for PPAR- $\gamma$  in macrophages infected with H99 and  $\Delta plb1$ . To quantify PPAR- $\gamma$  activation we measured its nuclear translocation by comparing nuclear and cytoplasmic fluorescence intensity in infected cells. PPAR- $\gamma$  is a cytosolic receptor that translocates to the nucleus upon activation, therefore cells where PPAR- $\gamma$  is activated should have increased nuclear staining for PPAR- $\gamma$ . We found that J774 macrophages infected with H99 had significantly higher levels of nuclear staining for PPAR- $\gamma$  compared to  $\Delta plb1$  infected

and uninfected cells (Fig 5A i and Supplementary Fig 3C). This confirmed that *C. neoformans* activates PPAR- $\gamma$  and that this phenotype is phospholipase B1 dependent.

To test the activation of PPAR- $\gamma$  during infection we first wanted to confirm that exogenous 15-keto-PGE<sub>2</sub> activates zebrafish PPAR- $\gamma$  *in vivo* by using transgenic PPAR- $\gamma$  reporter zebrafish larvae (36,37). We treated these larvae at 2 dpf with 15-keto-PGE<sub>2</sub> and Troglitazone (TLT) which is a specific agonist of PPAR- $\gamma$ . TLT treatment was performed with a concentration (0.55  $\mu$ M) previously shown to strongly activate PPAR- $\gamma$  in these zebrafish larvae (36). We found that TLT treatment at 2 dpf strongly activated GFP reporter expression in the larvae. We employed a receptor competition assay as a sensitive measurement of binding by simultaneously treating zebrafish with 15-keto-PGE<sub>2</sub> and TLT. We observed a reduction in GFP expression compared to TLT treatment alone (Fig 5 Aii), demonstrating competition for the same receptor. This could mean that 15-keto-PGE<sub>2</sub> was a partial agonist (38,39) or an antagonist to PPAR- $\gamma$  in this experiment. Existing studies suggest 15-keto-PGE<sub>2</sub> is an agonist to PPAR- $\gamma$  (32) but to confirm this in our model we treated  $\Delta plb1$ -GFP infected zebrafish larvae with exogenous 15-keto-PGE<sub>2</sub> as before but at the same time treated fish with the PPAR- $\gamma$  antagonist GW9662. We found that 15-keto-PGE<sub>2</sub> treatment significantly improved the growth of  $\Delta plb1$ -GFP during infection but that inhibition of PPAR- $\gamma$  was sufficient to reverse this effect (Fig 5C). Therefore, we could demonstrate that 15-keto-PGE<sub>2</sub> was an agonist to PPAR- $\gamma$ , and that PPAR- $\gamma$  activation was sufficient to promote a permissive environment for *C. neoformans* growth during infection.

To determine if PPAR- $\gamma$  activation by *C. neoformans* facilitates growth within macrophages we treated H99 and  $\Delta plb1$  infected J774 murine macrophages with the PPAR- $\gamma$  antagonist GW9662. GW9662 treatment significantly reduced the proliferation of H99, but not  $\Delta plb1$  (Fig

5B,  $p=0.026$ , 1.22-fold decrease vs. DMSO). Further supporting that PPAR- $\gamma$  activation is necessary for the successful intracellular parasitism of host macrophages by *C. neoformans*. Finally, to confirm that PPAR- $\gamma$  activation alone promoted *C. neoformans* infection we treated 2dpf infected zebrafish larvae with TLT at the same concentration known to activate PPAR- $\gamma$  in PPAR- $\gamma$  reporter fish (Fig 5A ii and (36)). We found that TLT treatment significantly increased the fungal burden of  $\Delta plb1$ -GFP (Fig 5E and,  $p = 0.0089$ , 1.68-fold increase vs. DMSO), H99-GFP (Fig 5D ,  $p = 0.0044$ , 1.46-fold increase vs. DMSO) and  $\Delta lac1$ -GFP (Fig 5F,  $p = 0.01$ , 1.94-fold increase vs. DMSO) infected larvae similar to 15-keto-PGE<sub>2</sub> treatment. Thus, we could show that host PPAR- $\gamma$  activation was sufficient to promote cryptococcal growth during infection and was a consequence of fungal derived prostaglandins.

## Discussion

We have shown for the first time that eicosanoids produced by *C. neoformans* promote fungal virulence both *in vitro* and *in vivo*. In this respect we have shown that the intracellular growth defects of two eicosanoid deficient *C. neoformans* strains  $\Delta plb1$  and  $\Delta lac1$  (21,23) can be rescued with the addition of exogenous PGE<sub>2</sub>. Furthermore, our *in vitro* co-infection assay, *in vitro* infection assays with aspirin, and *in vivo* infection assays provide evidence that the source of this eicosanoid during infection is from the pathogen, rather than the host. Using an *in vivo* zebrafish larvae model of cryptococcosis we find that that PGE<sub>2</sub> must be dehydrogenated into 15-keto-PGE<sub>2</sub> before to influence fungal growth. Finally, we provide evidence that the mechanism of PGE<sub>2</sub>/15-keto-PGE<sub>2</sub> mediated growth promotion during larval infection is via the activation of PPAR- $\gamma$  (33,34,40-42).

In a previous study it was identified that the *C. neoformans* mutant  $\Delta plb1$  (that lacks the *PLB1* gene coding for phospholipase B1) was deficient in replication and survival in macrophages (21), a phenotype also observed by a number of studies using different *in vitro* infection assays (19,23). In this study we demonstrate that supplementing  $\Delta plb1$  with exogenous prostaglandin E<sub>2</sub> during *in vitro* macrophages infection is sufficient to restore the mutant's intracellular proliferation defect. A key goal of this study was to investigate how eicosanoids produced by *C. neoformans* modulate pathogenesis *in vivo* (22). To facilitate *in vivo* measurement of fungal burden we created two GFP-tagged strains with constitutive GFP expression -  $\Delta plb1$ -GFP and  $\Delta lac1$ -GFP - to use alongside the GFP-tagged H99 parental strain previously produced (31). These two mutants are the only *C. neoformans* mutants known to have a deficiency in eicosanoid synthesis.  $\Delta plb1$  cannot produce any eicosanoid species suggesting phospholipase B1 is high in the eicosanoid synthesis pathway while  $\Delta lac1$  has a specific defect in PGE<sub>2</sub> suggesting it might be a prostaglandin E<sub>2</sub> synthase enzyme. To our knowledge these are the first GFP tagged versions of  $\Delta plb1$  and  $\Delta lac1$  created. Characterisation of  $\Delta plb1$ -GFP and



$\Delta lac1$ -GFP *in vivo* revealed that both strains have significantly reduced fungal burdens compared to H99-GFP. This is the first report of  $\Delta lac1$  in zebrafish but these observations do confirm a previous zebrafish study showing that non-fluorescent  $\Delta plb1$  had attenuated infectious burden in zebrafish larvae (43). To confirm that PGE<sub>2</sub> is also required for cryptococcal growth *in vivo* we treated  $\Delta plb1$ -GFP and  $\Delta lac1$ -GFP infected zebrafish larvae with exogenous PGE<sub>2</sub> to determine how it would affect fungal burden. In agreement with our *in vitro* findings we found that PGE<sub>2</sub> significantly improved the growth of both of these strains within larvae. Interestingly we also found that PGE<sub>2</sub> improved the growth of H99-GFP, perhaps representing a wider manipulation of host immunity during *in vivo* infection.

In vertebrate cells, PGE<sub>2</sub> is converted into 15-keto-PGE<sub>2</sub> by the enzyme 15-prostaglandin dehydrogenase (15PGDH), furthermore it has been reported that *C. neoformans* has enzymatic activity analogous to 15PGDH (18). To investigate how the dehydrogenation of PGE<sub>2</sub> to 15-keto-PGE<sub>2</sub> influenced fungal burden we treated infected larvae with 16,16-dm-PGE<sub>2</sub> – a synthetic variant of PGE<sub>2</sub> which is resistant to dehydrogenation (25). Interestingly we found that 16,16-dm-PGE<sub>2</sub> was unable to promote the growth of  $\Delta plb1$ -GFP, H99-GFP or  $\Delta lac1$ -GFP within infected larvae. These findings indicate that 15-keto-PGE<sub>2</sub>, rather than PGE<sub>2</sub>, promotes cryptococcal virulence. We subsequently treated infected larvae with exogenous 15-keto-PGE<sub>2</sub> and confirmed that 15-keto-PGE<sub>2</sub> treatment was sufficient to promote the growth of both  $\Delta plb1$ -GFP and H99-GFP, but not  $\Delta lac1$ -GFP (discussed below), without the need for PGE<sub>2</sub>. We therefore propose that PGE<sub>2</sub> produced by *C. neoformans* during infection must be enzymatically dehydrogenated into 15-keto-PGE<sub>2</sub> to promote cryptococcal virulence. These findings represent the identification of a new virulence factor (15-keto-PGE<sub>2</sub>) produced by *C. neoformans*, as well as the first-time identification of an eicosanoid other than PGE<sub>2</sub> with a role in promoting cryptococcal growth. Furthermore, our findings suggest that previous studies which identify

PGE<sub>2</sub> as a promoter of cryptococcal virulence (19,20,44) may have observed additive effects from both PGE<sub>2</sub> and 15-keto-PGE<sub>2</sub> activity.

Our experiments with the  $\Delta lac1$ -GFP strain reveals that this strain appears to respond in a similar way to PGE<sub>2</sub>, 16,16-dm-PGE<sub>2</sub> and troglitazone as  $\Delta plb1$ -GFP but appears to be unresponsive to 15-keto-PGE<sub>2</sub>. At this time, we cannot fully explain this phenotype,  $\Delta lac1$ -GFP was generally less responsive to PGE<sub>2</sub> and troglitazone treatments compared to  $\Delta plb1$ -GFP so it is possible that that higher concentrations of 15-keto-PGE<sub>2</sub> would be needed to rescue its growth defect, however experimentation with higher concentrations of 15-keto-PGE<sub>2</sub> led to significant host toxicity. The unresponsiveness of  $\Delta lac1$  to eicosanoid treatment could be due to unrelated virulence defects caused by laccase deficiency. Cryptococcal laccase expression is required for the production of fungal melanin – a well characterized virulence factor produced by *C. neoformans* (45,46). It is therefore likely that virulence defects unrelated to eicosanoid synthesis are responsible for the differences between the two mutant phenotypes.

We have found that the phospholipase B1 dependent attenuation of  $\Delta plb1$  can be rescued with the addition of exogenous PGE<sub>2</sub>. This indicates that synthesis and secretion of PGE<sub>2</sub> by *C. neoformans* is a virulence factor. Although our data indicated that *C. neoformans* was the source of PGE<sub>2</sub> we wanted exclude the possibility that host-derived PGE<sub>2</sub> was also contributing to virulence. To explore this possibility, we blocked host prostaglandin synthesis - we reasoned that if host PGE<sub>2</sub> was not required that blocking its production would not affect the growth of *C. neoformans*. To do this we first treated J774 macrophages infected with H99-GFP and  $\Delta plb1$ -GFP with aspirin – a cyclooxygenase inhibitor that blocks both COX-1 and COX-2 activity – and found that this had no effect on intracellular proliferation. Subsequently we attempted to block cyclooxygenase activity in zebrafish but found aspirin was lethal at the zebrafish larvae's currently stage of development, instead we used individual inhibitors specific for COX-1 (NS-398) and COX-2 (SC-560). We found that each inhibitor decreases fungal burden of H99-GFP

infected larvae but not  $\Delta plb1$ -GFP infected larvae. Due to the phospholipase B1 dependence of this phenotype we think that these inhibitors might be affecting eicosanoid production by the *C. neoformans* itself. The ability of broad COX inhibitors like aspirin/indomethacin to inhibit eicosanoid production by *C. neoformans* is controversial (17,28) however our study is the first to use such selective COX-1 and COX-2 inhibitors on *C. neoformans*. This experiment remained inconclusive as to whether host PGE<sub>2</sub> synthesis promotes virulence so to block PGE<sub>2</sub> in zebrafish larvae without potential off target effects we used CRISPR Cas9 technology to knockdown expression of the prostaglandin E<sub>2</sub> synthase gene *ptges* in zebrafish larvae. Ablating zebrafish *ptges* with this approach did not affect the fungal burden of  $\Delta plb1$ -GFP infected larvae but it did cause increased burden in H99-GFP infected zebrafish. This phenotype is interesting because it suggests host PGE<sub>2</sub> might actually be inhibitory to cryptococcal virulence, furthermore this phenotype was phospholipase B1 dependent which suggests host-derived PGE<sub>2</sub> might interact in some way with *Cryptococcus*-derived eicosanoids. This phenotype was not seen *in vitro* with aspirin so it is possible that the inhibitory effects of host-derived PGE<sub>2</sub> influence a non-macrophage cell type in zebrafish larvae.

To confirm our observations that *C. neoformans* was the source of PGE<sub>2</sub> during infection we performed co-infection assays with H99 wild type cryptococci (eicosanoid producing) and  $\Delta plb1$  (eicosanoid deficient) within the same macrophage and found that co-infection was sufficient to promote the intracellular growth of  $\Delta plb1$ . We also observed similar interactions during  $\Delta lac1$  co-infection (a second eicosanoid deficient *C. neoformans* mutant). These observations agree with previous studies that suggest eicosanoids are virulence factors produced by *C. neoformans* during macrophage infection (19,28). To identify if the secreted factor produced by *C. neoformans* was PGE<sub>2</sub>, we measured the levels of PGE<sub>2</sub> from *Cryptococcus* infected macrophages to see if there was an observable increase in this eicosanoid during infection. Although PGE<sub>2</sub> was detected, we did not see any significant difference between infected and

uninfected macrophages, an observation confirmed using two different detection techniques – ELISA and LC MS/MS. These data suggest that PGE<sub>2</sub> produced by *C. neoformans* during macrophage infection is contained within the macrophage, likely in close proximity to the fungus and that the host receptor targeted by these eicosanoids is therefore likely to be intracellular. Our *in vitro* co-infection experiments indicate that *C. neoformans* secretes virulence enhancing eicosanoids during infection.

The biological activity of 15-keto-PGE<sub>2</sub> is far less studied than PGE<sub>2</sub>. It is known that 15-keto-PGE<sub>2</sub> cannot bind to prostaglandin E<sub>2</sub> EP receptors, this means it can act as a negative regulator of PGE<sub>2</sub> activity i.e. cells up-regulate 15PGDH activity to lower PGE<sub>2</sub> levels (47). Our findings however suggested that 15-keto-PGE<sub>2</sub> did have a biological activity independent of PGE<sub>2</sub> synthesis, possibly via a distinct eicosanoid receptor. It has been demonstrated that 15-keto-PGE<sub>2</sub> can activate the intracellular eicosanoid receptor peroxisome proliferator associated receptor gamma (PPAR- $\gamma$ ) (32). Activation of PPAR- $\gamma$  by *C. neoformans* has not been described previously but it is compatible with what we know of cryptococcal pathogenesis. PPAR- $\gamma$  is a nuclear receptor normally found within the cytosol. Upon ligand binding PPAR- $\gamma$  forms a heterodimer with Retinoid X receptor (RXR) and translocates to the nucleus where it influences the expression of target genes which possess a peroxisome proliferation hormone response element (PPRE) (48). If eicosanoids are produced by *C. neoformans* during intracellular infection, it is likely that they bind to an intracellular eicosanoid receptor. Additionally, activation of PPAR- $\gamma$  within macrophages is known to promote the expression of anti-inflammatory genes which could make the macrophage more amenable to parasitism by the fungus.

To investigate whether PPAR- $\gamma$  activation within macrophages occurs during *C. neoformans* infection we performed immunofluorescent staining of H99 and  $\Delta plb1$  infected J774 macrophages. We found that infection with *C. neoformans* led to increased nuclear localization

of PPAR-  $\gamma$  indicating that the fungus was activating endogenous PPAR-  $\gamma$  during infection. We also found that macrophages infected with H99 had higher levels of PPAR-  $\gamma$  activation than  $\Delta plb1$  infected macrophages. This strongly suggests that eicosanoids produced by *C. neoformans* are responsible for activating PPAR-  $\gamma$ .

To confirm that 15-keto-PGE<sub>2</sub> is an agonist to PPAR- $\gamma$  we performed experiments with zebrafish larvae from PPAR- $\gamma$  GFP reporter fish (36) and demonstrated that 15-keto-PGE<sub>2</sub> binds to zebrafish PPAR-  $\gamma$ . To determine if 15-keto-PGE<sub>2</sub> is an agonist to PPAR-  $\gamma$  we found that treating  $\Delta plb1$ -GFP infected zebrafish larvae with GW9662 at the same time as 15-keto-PGE<sub>2</sub> blocked the virulence enhancing effects of the eicosanoid. These data indicate that 15-keto-PGE<sub>2</sub> is a partial agonist to PPAR- $\gamma$  (in zebrafish at least). Partial agonists are weak agonists that bind to and activate receptors, but not at the same efficacy as a full agonist. Partial agonists to PPAR- $\gamma$  have been reported previously, partial PPAR agonists bind to the ligand binding domain of PPAR- $\gamma$  with a lower affinity than full PPAR agonists and as a result activate smaller subsets of PPAR- $\gamma$  controlled genes (38,39,49-52).

We also found that activation of PPAR- $\gamma$  alone was sufficient to mediate cryptococcal virulence. In this respect, we found that the *in vitro* intracellular proliferation of the wild type H99 cryptococcal strain within J774 macrophages could be suppressed using a PPAR- $\gamma$  antagonist GW9662. We could also block the rescuing effect of 15-keto-PGE<sub>2</sub> on  $\Delta plb1$ -GFP during zebrafish infection using GW9662. Finally we found that *Cryptococcus* infected zebrafish treated with troglitazone at a concentration that is known to activate PPAR- $\gamma$  (53) had increased fungal burdens when infected with  $\Delta plb1$ -GFP,  $\Delta lac1$ -GFP and H99-GFP strains. Taken together these experiments provide convincing evidence that a novel cryptococcal virulence factor - 15-keto-PGE<sub>2</sub> – enhances the virulence of *C. neoformans* by activation of host PPAR- $\gamma$  and that macrophages are one of the key targets of this eicosanoid during infection.

In this study, we have shown for the first time that eicosanoids produced by *C. neoformans* can promote virulence in an *in vivo* host. Furthermore, we have provided evidence that this virulence occurs via eicosanoid mediated manipulation of host macrophages. We have identified that the eicosanoid responsible for these effects is 15-keto-PGE<sub>2</sub> which is derived from the dehydrogenation of PGE<sub>2</sub> produced by *C. neoformans*. We have subsequently demonstrated that 15-keto-PGE<sub>2</sub> mediates its effects via activation of PPAR-  $\gamma$ , an intracellular eicosanoid receptor known to promote anti-inflammatory immune pathways within macrophages. We provide compelling evidence that eicosanoids produced by *C. neoformans* enhance virulence, identifies a novel virulence factor – 15-keto-PGE<sub>2</sub> – and describes a novel mechanism of host manipulation by *C. neoformans* - activation of PPAR-  $\gamma$ . Most importantly this study provides a potential new therapeutic pathway for treatment of cryptococcal infection, as several eicosanoid modulating drugs are approved for patient treatment (54) .

## Materials and methods

(all reagents are from Sigma-Aldrich, UK unless otherwise stated)

## Ethics statement

Animal work was performed following UK law: Animal (Scientific Procedures) Act 1986, under Project License PPL 40/3574 and P1A4A7A5E. Ethical approval was granted by the University of Sheffield Local Ethical Review Panel. Experiments using the PPAR- $\gamma$  reporter fish line (53) were conducted at the University of Toronto following approved animal protocols (# 00000698 “A live zebrafish-based screening system for human nuclear receptor ligand and cofactor discovery”) under a OMAFRA certificate.

## Zebrafish

The following zebrafish strains were used for this study: *Nacre* wild type strain, *Tg(mpeg1:mCherryCAAX)sh378* transgenic strain and the double mutant *casper*, for PPAR $\gamma$  reporter experiments (53), which lacks all melanophores and iridophores (55). Zebrafish were maintained according to standard protocols. Adult fish were maintained on a 14:10 – hour light / dark cycle at 28 °C in UK Home Office approved facilities in the Bateson Centre aquaria at the University of Sheffield.

### ***C. neoformans***

The H99-GFP strain has been previously described (31). The  $\Delta plb1$ -GFP and  $\Delta lac1$ -GFP strains were generated for this study by transforming existing deletion mutant strains (23,56) with a GFP expression construct (see below for transformation protocol). All strains used are in the *C. neoformans* variety *grubii* H99 genetic background.

*Cryptococcus* strains were grown for 18 hours at 28 °C, rotating horizontally at 20 rpm. *Cryptococcus* cultures were pelleted at 3300g for 1 minute, washed twice with PBS (Oxoidm Basingstoke, UK) and re-suspended in 1ml PBS. Washed cells were then counted with a haemocytometer and used as described below.

### ***C. neoformans* transformation**

*C. neoformans* strains  $\Delta plb1$  and  $\Delta lac1$  were biolistically transformed using the pAG32\_GFP transformation construct as previously described for H99-GFP (31). Stable transformants were identified by passaging positive GFP fluorescent colonies for at least 3 passages on YPD agar supplemented with 250  $\mu$ g/ml Hygromycin B.

### **Zebrafish CRISPR**

CRISPR generation was performed as previously described (29). Briefly gRNA spanning the ATG start codon of zebrafish *ptges* or *tyr* was injected along with Cas9 protein and tracrRNA

into zebrafish embryos at the single cell stage. Crispant larvae were infected with *C. neoformans* as described above at 2 dpf. The genotype of each larvae was confirmed post assay – genomic DNA was extracted from each larvae and the ATG was PCR amplified with primers spanning the ATG site of *ptges* (Forward primer gccagtgataatgaggaatggg, Reverse primer aatgtttggattaaacgcgact) producing a 345-bp product. This product was digested with MwoI – wildtype digests produced bands at 184, 109 and 52 bp while mutant digests produced bands at 293 and 52 bp (Supplementary Figure 4).

#### **J774 Macrophage infection – with exogenous PGE<sub>2</sub> treatment**

J774 macrophage (J774 cells were obtained from the ATCC, American Type Culture Collection) infection was performed as previously described (21) with the following alterations. J774 murine macrophage-like cells were cultured for a minimum of 4 passages in T75 tissue culture flasks at 37°C 5% CO<sub>2</sub> in DMEM (High glucose, Sigma) supplemented with 10% Fetal Bovine Calf Serum (Invitrogen), 1% 10,000 units Penicillin / 10 mg streptomycin and 1 % 200 mM L – glutamine, fully confluent cells were used for each experiment. Macrophages were counted by haemocytometer and diluted to a concentration of 1x10<sup>5</sup> cells per ml in DMEM supplemented with 1 µg/ml lipopolysaccharide (LPS from *E. coli*, Sigma L2630) before being plated into 24 well microplates (Greiner) and incubated for 24 hours (37 °C 5% CO<sub>2</sub>).

Following 24-hour incubation, medium was removed and replaced with 1 ml DMEM supplemented with 2 nM prostaglandin E<sub>2</sub> (CAY14010, 1mg/ml stock in 100% ethanol). Macrophage wells were then infected with 100 µl 1x10<sup>6</sup> yeast/ml *Cryptococcus* cells (from overnight culture, washed. See above) opsonized with anti-capsular IgG monoclonal antibody (18b7, a kind gift from Arturo Casadevall). Cells were incubated for 2 hours (37 °C 5% CO<sub>2</sub>) and then washed with 37 °C PBS until extracellular yeast were removed. After washing, infected cells were treated with 1ml DMEM supplemented with PGE<sub>2</sub>.



To calculate IPR, replicate wells for each treatment/strain were counted at 0 and 18 hours. Each well was washed once with 1ml 37 °C PBS prior to counting to remove any *Cryptococcus* cells released by macrophage death or vomocytosis. Intra-macrophage Cryptococci were released by lysis with 200 µl dH<sub>2</sub>O for 20 minutes (lysis confirmed under microscope). Lysate was removed to a clean microcentrifuge tube and an additional 200 µl was used to wash the well to make a total lysate volume of 400 µl. *Cryptococcus* cells within lysates were counted by haemocytometer. IPR was calculated by dividing the total number of counted yeast at 18hr by the total at 0hr.

To assess the viability of *C. neoformans* cells recovered from macrophages we used our previously published colony forming unit (CFU) viability assay (21). Lysates from *C. neoformans* infected J774 cells were prepared from cells at 0hr and 18hr time points. The concentration of *C. neoformans* cells in the lysate was calculated by haemocytometer counting, the lysates were then diluted to give an expected concentration of  $2 \times 10^3$  yeast cells per ml. 100 µl of this diluted lysate was spread onto a YPD agar plate and incubated for 48 hr at 25°C prior to colony counting.

#### **J774 Macrophage co-infection.**

J774 cells were prepared and seeded at a concentration of  $1 \times 10^5$  per ml as above in 24 well microplates and incubated for 24 hours (37 °C 5% CO<sub>2</sub>), 45 minutes prior to infection J774 cells were activated with 150 ng/ml phorbol 12-myristate 13-acetate in DMSO added to 1 ml serum free DMEM. Following activation J774 cells were washed and infected with 100 µl /  $1 \times 10^6$  yeast/ml 50:50 mix of  $\Delta plb1$  (non-fluorescent) and H99-GFP (e.g.  $5 \times 10^5$   $\Delta plb1$  and  $5 \times 10^5$  H99-GFP) or  $\Delta lac1$ -GFP and H99 (non-fluorescent). Infected cells were incubated for 2 hours (37 °C 5% CO<sub>2</sub>) to allow for phagocytosis of *Cryptococcus* and then washed multiple times with 37 °C

PBS to remove unphagocytosed yeast, each well was observed between washes to ensure that macrophages were not being washed away. After washing 1 ml DMEM was added to each well. Co-infected cells were imaged over 20 hours using a Nikon TE2000 microscope fitted with a climate controlled incubation chamber (37 °C 5% CO<sub>2</sub>) using a Digital Sight DS-QiMC camera and a Plan APO Ph1 20x objective lens (Nikon). GFP and bright field images were captured every 4 minutes for 20 hours. Co-infection movies were scored manually. For example co-infected macrophages that contained 2  $\Delta plb1$  (non-fluorescent) and 1 H99-GFP (GFP positive) yeast cells at 0 hr were tracked for 18 hours and before the burden of each strain within the macrophage was counted again. The IPR for  $\Delta plb1$  within co-infected macrophages was calculated by dividing the number of  $\Delta plb1$  cells within a macrophage at 18 hr by the number at 0 hr.

## Immunofluorescence

J774 cells were cultured to confluency as discussed above and seeded onto sterile 13 mm glass coverslips at a density of 10<sup>5</sup> cells per ml without activation by phorbol 12-myristate 13-acetate. H99-GFP and  $\Delta plb1$ -GFP were opsonised with 18B7 for one hour. 18B7 was then removed by centrifugation and fungal cells were suspended in 1 ml of PBS with 1:200 FITC for one hour. Supernatant was removed again, cells were resuspended in PBS, and J774 were infected with 10<sup>6</sup> of either H99-GFP or  $\Delta plb1$ -GFP in serum free DMEM. After two hours of infection media was removed from J774s and the J774s were washed three times with PBS. 10  $\mu$ m TLT or DMSO was added to uninfected cells to act as controls. Cells were then left for 18 hours at 37 °C 5 % CO<sub>2</sub>.

After 18 hours supernatants were removed and J774s were fixed with cold methanol for 5 minutes at -20 °C before washing with PBS three times, leaving PBS for five minutes at room temperature between washes. Coverslips were blocked with 5% sheep serum in 0.1% triton

(block solution) for 20 minutes before being transferred into the primary PPAR- $\gamma$  antibody (1:50, Santa Cruz Biotechnology sc-7273 lot #B1417) with 1:10 human IgG in block solution for one hour. Coverslips were washed 3 times in PBS and incubated with 1:200 anti-mouse TRITC, 1:40 anti-human IgG, and 0.41  $\mu$ l/ml DAPI in block solution for one hour. Coverslips were then washed three times with PBS, three times with water, and fixed to slides using MOWIOL. Slides were left in the dark overnight and imaged the following day. Imaging was performed on a Nikon Eclipse Ti microscope with a x60 DIC objective. Cells were imaged with filter sets for Cy3 (PPAR- $\gamma$  , 500ms exposure) GFP (*Cryptococcus*, 35 ms exposure) and DAPI (Nuclei, 5ms) dyes in addition to DIC.

The intensity of nuclear staining was analysed for at least 30 cells per coverslip, using ImageJ 2.0.0 a line ROI was drawn from the outside of cell, through the nucleus measuring the mean grey value along the line. For *Cryptococcus* infected conditions uninfected and infected cells were measured separately upon the same coverslip using the GFP channel to distinguish between infected and uninfected cells.

### **J774 aspirin timelapse**

Macrophages were seeded at  $10^5$  per ml into 24 well plates as described above. After two hours cells requiring aspirin were treated with 1 mM aspirin in DMSO in fresh DMEM. Cells were then incubated overnight for 18 hours at 37 °C 5% CO<sub>2</sub>. H99-GFP and  $\Delta$ *plb1*-GFP were prepared at  $10^6$  cells per ml as described above, and opsonised with 18B7 for one hour. J774s were then infected with the fungal cells in fresh serum free DMEM for two hours before removing the supernatant, washing three times in PBS, and adding fresh serum free DMEM. Cells were imaged for 18 hours on a Nikon Eclipse Ti equipped with a climate controlled stage (Temperature - 37 °C, Atmosphere - 5% CO<sub>2</sub> / 95% air) with a x20 Lambda Apo NA 0.75 phase

contrast objective brightfield images were taken at an interval of 2 minutes, 50 ms exposure. Analysis was performed by manual counts of intracellular and extracellular cryptococci.

# **Zebrafish infection**

Washed and counted *Cryptococcus* cells from overnight culture were pelleted at 3300g for 1 minute and re-suspended in 10% Polyvinylpyrrolidone (PVP), 0.5% Phenol Red in PBS to give the required inoculum in 1 nl. This injection fluid was loaded into glass capillaries shaped with a needle puller for microinjection. Zebrafish larvae were injected at 2-days post fertilisation; the embryos were anaesthetised by immersion in 0.168 mg/ml tricaine in E3 before being transferred onto microscope slides coated with 3% methyl cellulose in E3 for injection. Prepared larvae were injected with two 0.5 nl boluses of injection fluid by compressed air into the yolk sac circulation valley. Following injection, larvae were removed from the glass slide and transferred to E3 to recover from anaesthetic and then transferred to fresh E3 to remove residual methyl cellulose. Successfully infected larvae (displaying systemic infection throughout the body and no visible signs of damage resulting from injection) were sorted using a fluorescent stereomicroscope. Infected larvae were maintained at 28 °C.

# **Eicosanoid / receptor agonist treatment of infected zebrafish larvae**

All compounds were purchased from Cayman Chemical. Compounds were resuspended in DMSO and stored at -20 °C until used. Prostaglandin E<sub>2</sub> (CAY14010, 10mg/ml stock), Prostaglandin D<sub>2</sub> (CAY12010, 10mg/ml stock), 16,16-dimethyl-PGE<sub>2</sub> (CAY14750, 10mg/ml stock), 15-keto-PGE<sub>2</sub> (CAY14720, 10mg/ml stock), troglitazone (CAY14720, 10mg/ml stock), GW9662 (CAY70785, 1mg/ml stock), AH6809 (CAY14050, 1mg/ml stock), GW627368X (CAY10009162, 10mg/ml stock), NS-398 (CAY70590, 9.4mg/ml stock), SC-560 (CAY70340, 5.3mg/ml stock).

Treatment with exogenous compounds during larval infected was performed by adding compounds (or equivalent solvent) to fish water (E3) to achieve the desired concentration. Fish were immersed in compound supplemented E3 throughout the experiment from the time of injection.

### **Zebrafish fungal burden measurement**

Individual infected zebrafish embryos were placed into single wells of a 96 well plate (VWR) with 200  $\mu$ l of E3 (unsupplemented E3, or E3 supplemented with eicosanoids / drugs depending on the assay). Infected embryos were imaged at 0 days post infection (dpi), 1 dpi, 2 dpi and 3 dpi in their 96 well plates using a Nikon Ti-E with a CFI Plan Achromat UW 2X N.A 0.06 objective lens. Images were captured with a Neo sCMOS (Andor, Belfast, UK) and NIS Elements (Nikon, Richmond, UK). Images were exported from NIS Elements into Image J FIJI as monochrome tif files. Images were thresholded in FIJI using the 'moments' threshold preset and converted to binary images to remove all pixels in the image that did not correspond to the intensity of the fluorescently tagged *C. neoformans*. The outline of the embryo was traced using the 'polygon' ROI tool, avoiding autofluorescence from the yolk sac. The total number of pixels in the thresholded image were counted using the FIJI 'analyse particles' function, the 'total area' measurement from the 'summary' readout was used for the total number of GFP<sup>+</sup> pixels in each embryo.

### **PPAR- $\gamma$ GFP reporter fish treatment**

PPAR $\gamma$  embryos were collected from homozygous ligand trap fish (F18). Embryos were raised in a temperature-controlled water system under LD cycle at 28.5° C. in 0.5 $\times$ E2 media in petri-dishes till 1 dpf. Any developmentally delayed (dead or unfertilized) embryos were removed. Chorions were removed enzymatically with Pronase (1mg/ml) and specimens were dispensed into 24 well plates (10 per well) in 0.5 $\times$ E2 media. For embryos 1% DMSO was used as a vehicle

control. Chemicals were stored in DMSO, diluted appropriately and added individually to 400 ul of 0.5×E2 media with 0.05 U/ml penicillin and 50 ng/ml streptomycin and vortexed intensively for 1 min. 0.5×E2 media was removed from all wells with embryos and the 400 ul chemical solutions were administered to different wells to embryos. For drug treatment embryos were pre-incubated for 1 hour with compounds and then heat induced (28→37° C.) for 30 min in a water bath. Embryos were incubated at 28°C for 18 h and then monitored using a fluorescent dissection scope (SteREO Lumar.V12 Carl Zeiss) at 2 dpf. For analyzing GFP fluorescent pattern, embryos were anesthetized with Tricaine (Sigma, Cat.# A-5040) and mounted in 2 % methyl cellulose.

### **Whole body macrophage counts**

2 dpf transgenic zebrafish larvae which have fluorescently tagged macrophages due to an mCherry fluorescent protein driven by the macrophage specific gene marker *mpeg1* (57) *Tg(mpeg1:mCherryCAAX)sh378* (22) were treated with 10 μM PGE<sub>2</sub>, 10 μM 15-keto-PGE<sub>2</sub> or an equivalent DMSO control for 2 days. Larvae were then anesthetized by immersion in 0.168 mg/ml tricaine in E3 and imaged using a Nikon Ti-E with a Nikon Plan APO 20x/ 0.75 DIC N2 objective lens, taking z stacks of the entire body with 15 μm z steps. Macrophage counts were made manually using ImageJ from maximum projections.

### **Eicosanoid measurement (ELISA)**

J774 macrophages were seeded into 24 well plates at a concentration of 1×10<sup>5</sup> per well and incubated for 24 hours at 37 °C 5 % CO<sub>2</sub>. J774 cells were infected with *C. neoformans* as described above, at the same MOI 1:10 and incubated for 18 hours with 1ml serum free DMEM. At 18 hours post infection the supernatant was removed for ELISA analysis.

For ELISA analysis with aspirin treatment, wells requiring aspirin had supernatants removed and replaced with fresh DMEM containing 1mM aspirin in 1% DMSO. Cells were left for 24

hours total. At 24 hours all wells received fresh serum free media. Wells requiring aspirin for the duration received 1mM aspirin in DMSO. Aspirin treated cells requiring arachidonic acid were treated with 30 µg per ml arachidonic acid in ethanol. Control wells received the following: either 1% DMSO, 30 µg per ml arachidonic acid, or ethanol. Cells were again left at 37 °C 5 % CO<sub>2</sub> for 18 hours.

Supernatants were then removed and frozen at -80 °C until use. Supernatants were analysed as per the PGE<sub>2</sub> EIA ELISA kit instructions (Cayman Chemical).

### **Eicosanoid measurement (Mass spectrometry)**

J774 macrophages were seeded into T25 tissue culture flasks at a concentration of 1.3x10<sup>6</sup> cells per flask and incubated for 24 hours at 37 °C 5 % CO<sub>2</sub>. J774 cells were infected with *C. neoformans* as described above, at the same MOI 1:10 and incubated for 18 hours with 2 ml serum free DMEM. At 18 hours post infection infected cells were scraped from the flask with a cell scraper into the existing supernatant and immediately snap frozen in ethanol / dry ice slurry. All samples were stored at -80 °C before analysis.

Lipids and lipid standards were purchased from Cayman Chemical (Ann Arbor, Michigan). Deuterated standard Prostaglandin E<sub>2</sub>-d<sub>4</sub> (PGE<sub>2</sub>-d<sub>4</sub>), ≥98% deuterated form. HPLC grade solvents were from Thermo Fisher Scientific (Hemel Hempstead, Hertfordshire UK).

Lipids were extracted by adding a solvent mixture (1 mol/L acetic acid, isopropyl alcohol, hexane (2:20:30, v/v/v)) to the sample at a ratio of 2.5 –1 ml sample, vortexing, and then adding 2.5 ml of hexane (58). Where quantitation was required, 2 ng PGE<sub>2</sub>-d<sub>4</sub>, was added to samples before extraction, as internal standard. After vortexing and centrifugation, lipids were recovered in the upper hexane layer. The samples were then re-extracted by addition of an equal volume of hexane. The combined hexane layers were dried and analyzed for Prostaglandin E<sub>2</sub> (PGE<sub>2</sub>) using LC-MS/MS as below.

Lipid extracts were separated by reverse-phase HPLC using a ZORBAX RRHD Eclipse Plus 95Å C18, 2.1 x 150 mm, 1.8 µm column (Agilent Technologies, Cheshire, UK), kept in a column oven maintained at 45°C. Lipids were eluted with a mobile phase consisting of A, water-B-acetic acid of 95:5:0.01 (vol/vol/vol), and B, acetonitrile-methanol-acetic acid of 80:15:0.01 (vol/vol/vol), in a gradient starting at 30% B. After 1 min that was ramped to 35% over 3 min, 67.5% over 8.5 min and to 100% over 5 min. This was subsequently maintained at 100% B for 3.5 min and then at 30% B for 1.5 min, with a flow rate of 0.5 ml/min. Products were monitored by LC/MS/MS in negative ion mode, on a 6500 Q-Trap (Sciex, Cheshire, United Kingdom) using parent-to-daughter transitions of  $m/z$  351.2 → 271.2 (PGE<sub>2</sub>), and  $m/z$  355.2 → 275.2 for PGE<sub>2</sub>-d<sub>4</sub>. ESI-MS/MS conditions were: TEM 475 °C, GS1 60, GS2 60, CUR 35, IS -4500 V, dwell time 75 s, DP -60 V, EP -10 V, CE -25 V and CXP at -10 V. PGE<sub>2</sub> was quantified using standard curves generated by varying PGE<sub>2</sub> with a fixed amount of PGE<sub>2</sub>-d<sub>4</sub>.

## Acknowledgments

We thank the Bateson Centre aquaria staff for their assistance with zebrafish husbandry and the Johnston, Renshaw and Elks labs for critical discussions. We also thank Arturo Casadevall (Johns Hopkins University, Maryland USA) for providing the 18B7 antibody.



- 747 (1) Brown GD, Denning DW, Gow NA, Levitz SM, Netea MG, White TC. Hidden killers: human  
748 fungal infections. *Sci Transl Med* 2012 Dec 19;4(165):165rv13.
- 749 (2) Rajasingham R, Smith RM, Park BJ, Jarvis JN, Govender NP, Chiller TM, et al. Global  
750 burden of disease of HIV-associated cryptococcal meningitis: an updated analysis. *Lancet Infect*  
751 *Dis* 2017 May 5.
- 752 (3) Kawakami K, Kohno S, Kadota J, Tohyama M, Teruya K, Kudeken N, et al. T cell-dependent  
753 activation of macrophages and enhancement of their phagocytic activity in the lungs of mice  
754 inoculated with heat-killed *Cryptococcus neoformans*: involvement of IFN-gamma and its  
755 protective effect against cryptococcal infection. *Microbiol Immunol* 1995;39(2):135-143.
- 756 (4) Voelz K, Lammas DA, May RC. Cytokine signaling regulates the outcome of intracellular  
757 macrophage parasitism by *Cryptococcus neoformans*. *Infect Immun* 2009 Aug;77(8):3450-3457.
- 758 (5) Leopold Wager CM, Hole CR, Wozniak KL, Olszewski MA, Wormley FL, Jr. STAT1 signaling  
759 is essential for protection against *Cryptococcus neoformans* infection in mice. *J Immunol* 2014  
760 Oct 15;193(8):4060-4071.
- 761 (6) Chrétien F, Lortholary O, Kansau I, Neuville S, Gray F, Dromer F. Pathogenesis of cerebral  
762 *Cryptococcus neoformans* infection after fungemia. *J Infect Dis* 2002 Aug;186:522-530.
- 763 (7) Charlier C, Nielsen K, Daou S, Brigitte M, Chretien F, Dromer F. PMC2612285; Evidence of  
764 a role for monocytes in dissemination and brain invasion by *Cryptococcus neoformans*. *Infect*  
765 *Immun* 2009 Jan;77:120-127.
- 766 (8) Gilbert AS, Seoane PI, Sephton-Clark P, Bojarczuk A, Hotham R, Giurisato E, et al.  
767 Vomocytosis of live pathogens from macrophages is regulated by the atypical MAP kinase  
768 ERK5. *Sci Adv* 2017 08/16;3(8).
- 769 (9) Smith LM, Dixon EF, May RC. The fungal pathogen *Cryptococcus neoformans* manipulates  
770 macrophage phagosome maturation. *Cell Microbiol* 2015 May;17(5):702-713.
- 771 (10) Norris PC, Reichart D, Dumlao DS, Glass CK, Dennis EA. Specificity of eicosanoid  
772 production depends on the TLR-4-stimulated macrophage phenotype. *J Leukoc Biol* 2011  
773 Sep;90(3):563-574.
- 774 (11) Gupta S, Maurya MR, Stephens DL, Dennis EA, Subramaniam S. An integrated model of  
775 eicosanoid metabolism and signaling based on lipidomics flux analysis. *Biophys J* 2009 Jun  
776 3;96(11):4542-4551.
- 777 (12) Harizi H. The immunobiology of prostanoid receptor signaling in connecting innate and  
778 adaptive immunity. *Biomed Res Int* 2013;2013:683405.
- 779 (13) Angeli V, Faveeuw C, Roye O, Fontaine J, Teissier E, Capron A, et al. Role of the parasite-  
780 derived prostaglandin D2 in the inhibition of epidermal Langerhans cell migration during  
781 schistosomiasis infection. *J Exp Med* 2001 May 21;193(10):1135-1147.

- 782 (14) Ahmadi M, Emery DC, Morgan DJ. Prevention of both direct and cross-priming of antitumor  
783 CD8+ T-cell responses following overproduction of prostaglandin E2 by tumor cells in vivo.  
784 Cancer Res 2008 Sep 15;68(18):7520-7529.
- 785 (15) Harizi H, Corcuff JB, Gualde N. Arachidonic-acid-derived eicosanoids: roles in biology and  
786 immunopathology. Trends Mol Med 2008 Oct;14:461-469.
- 787 (16) Noverr MC, Erb-Downward JR, Huffnagle GB. Production of eicosanoids and other  
788 oxylipins by pathogenic eukaryotic microbes. Clin Microbiol Rev 2003 Jul;16(3):517-533.
- 789 (17) Erb-Downward JR, Huffnagle GB. Cryptococcus neoformans produces authentic  
790 prostaglandin E2 without a cyclooxygenase. Eukaryot Cell 2007 Feb;6(2):346-350.
- 791 (18) Erb-Downward JR, Noggle RM, Williamson PR, Huffnagle GB. The role of laccase in  
792 prostaglandin production by Cryptococcus neoformans. Mol Microbiol 2008 Jun;68(6):1428-  
793 1437.
- 794 (19) Noverr MC, Cox GM, Perfect JR, Huffnagle GB. PMC148814; Role of PLB1 in pulmonary  
795 inflammation and cryptococcal eicosanoid production. Infect Immun 2003 Mar;71:1538-1547.
- 796 (20) Shen L, Liu Y. Prostaglandin E2 blockade enhances the pulmonary anti-Cryptococcus  
797 neoformans immune reaction via the induction of TLR-4. Int Immunopharmacol 2015  
798 Sep;28(1):376-381.
- 799 (21) Evans RJ, Li Z, Hughes WS, Djordjevic JT, Nielsen K, May RC. Cryptococcal  
800 Phospholipase B1 (Plb1) is required for intracellular proliferation and control of titan cell  
801 morphology during macrophage infection. Infect Immun 2015 Jan 20.
- 802 (22) Bojarczuk A, Miller KA, Hotham R, Lewis A, Ogryzko NV, Kamuyango AA, et al.  
803 Cryptococcus neoformans Intracellular Proliferation and Capsule Size Determines Early  
804 Macrophage Control of Infection. Sci Rep 2016 Feb 18;6:21489.
- 805 (23) Cox GM, McDade HC, Chen SC, Tucker SC, Gottfredsson M, Wright LC, et al. Extracellular  
806 phospholipase activity is a virulence factor for Cryptococcus neoformans. Mol Microbiol 2001  
807 Jan;39:166-175.
- 808 (24) Chayakulkeeree M, Johnston SA, Oei JB, Lev S, Williamson PR, Wilson CF, et al. SEC14  
809 is a specific requirement for secretion of phospholipase B1 and pathogenicity of Cryptococcus  
810 neoformans. Mol Microbiol 2011 May;80:1088-1101.
- 811 (25) Ohno H, Morikawa Y, Hirata F. Studies on 15-hydroxyprostaglandin dehydrogenase with  
812 various prostaglandin analogues. J Biochem 1978 Dec;84(6):1485-1494.
- 813 (26) North TE, Goessling W, Walkley CR, Lengerke C, Kopani KR, Lord AM, et al.  
814 Prostaglandin E2 regulates vertebrate haematopoietic stem cell homeostasis. Nature 2007 Jun  
815 21;447(7147):1007-1011.
- 816 (27) Ricciotti E, FitzGerald GA. Prostaglandins and inflammation. Arterioscler Thromb Vasc Biol  
817 2011 May;31(5):986-1000.

- 818 (28) Noverr MC, Phare SM, Toews GB, Coffey MJ, Huffnagle GB. Pathogenic yeasts  
819 *Cryptococcus neoformans* and *Candida albicans* produce immunomodulatory prostaglandins.  
820 *Infect Immun* 2001 May;69(5):2957-2963.
- 821 (29) Loynes CA, Lee JA, Robertson AL, Steel MJ, Ellett F, Feng Y, et al. PGE2 production at  
822 sites of tissue injury promotes an anti-inflammatory neutrophil phenotype and determines the  
823 outcome of inflammation resolution in vivo. *Sci Adv* 2018 Sep 5;4(9):eaar8320.
- 824 (30) Voelz K, Johnston SA, Smith LM, Hall RA, Idnurm A, May RC. 'Division of labour' in  
825 response to host oxidative burst drives a fatal *Cryptococcus gattii* outbreak. *Nat Commun* 2014  
826 Oct 17;5:5194.
- 827 (31) Voelz K, Johnston SA, Rutherford JC, May RC. Automated analysis of cryptococcal  
828 macrophage parasitism using GFP-tagged cryptococci. *PLoS One* 2010 Dec 31;5(12):e15968.
- 829 (32) Chou WL, Chuang LM, Chou CC, Wang AH, Lawson JA, FitzGerald GA, et al. Identification  
830 of a novel prostaglandin reductase reveals the involvement of prostaglandin E2 catabolism in  
831 regulation of peroxisome proliferator-activated receptor gamma activation. *J Biol Chem* 2007  
832 Jun 22;282(25):18162-18172.
- 833 (33) Alleva DG, Johnson EB, Lio FM, Boehme SA, Conlon PJ, Crowe PD. Regulation of murine  
834 macrophage proinflammatory and anti-inflammatory cytokines by ligands for peroxisome  
835 proliferator-activated receptor-gamma: counter-regulatory activity by IFN-gamma. *J Leukoc Biol*  
836 2002 Apr;71(4):677-685.
- 837 (34) Maggi LB, Jr, Sadeghi H, Weigand C, Scarim AL, Heitmeier MR, Corbett JA. Anti-  
838 inflammatory actions of 15-deoxy-delta 12,14-prostaglandin J2 and troglitazone: evidence for  
839 heat shock-dependent and -independent inhibition of cytokine-induced inducible nitric oxide  
840 synthase expression. *Diabetes* 2000 Mar;49(3):346-355.
- 841 (35) Jiang C, Ting AT, Seed B. PPAR-gamma agonists inhibit production of monocyte  
842 inflammatory cytokines. *Nature* 1998 Jan;391:82-86.
- 843 (36) Tiefenbach J, Moll PR, Nelson MR, Hu C, Baev L, Kislinger T, et al. A live zebrafish-based  
844 screening system for human nuclear receptor ligand and cofactor discovery. *PLoS One* 2010  
845 Mar 22;5(3):e9797.
- 846 (37) Tiefenbach J, Magomedova L, Liu J, Reunov AA, Tsai R, Eappen NS, et al. Idebenone and  
847 coenzyme Q10 are novel PPARalpha/gamma ligands, with potential for treatment of fatty liver  
848 diseases. *Dis Model Mech* 2018 Aug 31;11(9):10.1242/dmm.034801.
- 849 (38) Atanasov AG, Wang JN, Gu SP, Bu J, Kramer MP, Baumgartner L, et al. Honokiol: a non-  
850 adipogenic PPARgamma agonist from nature. *Biochim Biophys Acta* 2013 Oct;1830(10):4813-  
851 4819.
- 852 (39) Bhalla K, Hwang BJ, Choi JH, Dewi R, Ou L, Mclenithan J, et al. N-Acetylfarnesylcysteine  
853 is a novel class of peroxisome proliferator-activated receptor gamma ligand with partial and full  
854 agonist activity in vitro and in vivo. *J Biol Chem* 2011 Dec 2;286(48):41626-41635.

- 855 (40) Bouhlef MA, Derudas B, Rigamonti E, Dievart R, Brozek J, Haulon S, et al. PPARgamma  
856 activation primes human monocytes into alternative M2 macrophages with anti-inflammatory  
857 properties. *Cell Metab* 2007 Aug;6(2):137-143.
- 858 (41) Bonfield TL, Thomassen MJ, Farver CF, Abraham S, Koloze MT, Zhang X, et al.  
859 Peroxisome proliferator-activated receptor-gamma regulates the expression of alveolar  
860 macrophage macrophage colony-stimulating factor. *J Immunol* 2008 Jul 1;181(1):235-242.
- 861 (42) Odegaard JI, Ricardo-Gonzalez RR, Goforth MH, Morel CR, Subramanian V, Mukundan L,  
862 et al. Macrophage-specific PPARgamma controls alternative activation and improves insulin  
863 resistance. *Nature* 2007 Jun 28;447(7148):1116-1120.
- 864 (43) Tenor JL, Oehlers SH, Yang JL, Tobin DM, Perfect JR. Live Imaging of Host-Parasite  
865 Interactions in a Zebrafish Infection Model Reveals Cryptococcal Determinants of Virulence and  
866 Central Nervous System Invasion. *MBio* 2015 Sep 29;6(5):e01425-15.
- 867 (44) Valdez PA, Vithayathil PJ, Janelins BM, Shaffer AL, Williamson PR, Datta SK.  
868 Prostaglandin E2 suppresses antifungal immunity by inhibiting interferon regulatory factor 4  
869 function and interleukin-17 expression in T cells. *Immunity* 2012 Apr 20;36(4):668-679.
- 870 (45) Salas SD, Bennett JE, Kwon-Chung KJ, Perfect JR, Williamson PR. Effect of the laccase  
871 gene CNLAC1, on virulence of *Cryptococcus neoformans*. *J Exp Med* 1996 Aug 1;184(2):377-  
872 386.
- 873 (46) Qiu Y, Davis MJ, Dayrit JK, Hadd Z, Meister DL, Osterholzer JJ, et al. Immune modulation  
874 mediated by cryptococcal laccase promotes pulmonary growth and brain dissemination of  
875 virulent *Cryptococcus neoformans* in mice. *PLoS One* 2012;7(10):e47853.
- 876 (47) Coggins KG, Latour A, Nguyen MS, Audoly L, Coffman TM, Koller BH. Metabolism of  
877 PGE2 by prostaglandin dehydrogenase is essential for remodeling the ductus arteriosus. *Nat*  
878 *Med* 2002 Feb;8(2):91-92.
- 879 (48) Lemberger T, Desvergne B, Wahli W. Peroxisome proliferator-activated receptors: a  
880 nuclear receptor signaling pathway in lipid physiology. *Annu Rev Cell Dev Biol* 1996;12:335-  
881 363.
- 882 (49) Pochetti G, Godio C, Mitro N, Caruso D, Galmozzi A, Scurati S, et al. Insights into the  
883 mechanism of partial agonism: crystal structures of the peroxisome proliferator-activated  
884 receptor gamma ligand-binding domain in the complex with two enantiomeric ligands. *J Biol*  
885 *Chem* 2007 Jun 8;282(23):17314-17324.
- 886 (50) Bruning JB, Chalmers MJ, Prasad S, Busby SA, Kamenecka TM, He Y, et al. Partial  
887 agonists activate PPARgamma using a helix 12 independent mechanism. *Structure* 2007  
888 Oct;15(10):1258-1271.
- 889 (51) Guasch L, Sala E, Castell-Auvi A, Cedo L, Liedl KR, Wolber G, et al. Identification of  
890 PPARgamma partial agonists of natural origin (I): development of a virtual screening procedure  
891 and in vitro validation. *PLoS One* 2012;7(11):e50816.

892 (52) Burgermeister E, Schnoebelen A, Flament A, Benz J, Stihle M, Gsell B, et al. A novel  
893 partial agonist of peroxisome proliferator-activated receptor-gamma (PPARgamma) recruits  
894 PPARgamma-coactivator-1alpha, prevents triglyceride accumulation, and potentiates insulin  
895 signaling in vitro. *Mol Endocrinol* 2006 Apr;20(4):809-830.

896 (53) Tiefenbach J, Moll PR, Nelson MR, Hu C, Baev L, Kislinger T, et al. A live zebrafish-based  
897 screening system for human nuclear receptor ligand and cofactor discovery. *PLoS One* 2010  
898 Mar 22;5(3):e9797.

899 (54) Day RO, Graham GG. Non-steroidal anti-inflammatory drugs (NSAIDs). *BMJ* 2013 Jun  
900 11;346:f3195.

901 (55) White RM, Sessa A, Burke C, Bowman T, LeBlanc J, Ceol C, et al. Transparent adult  
902 zebrafish as a tool for in vivo transplantation analysis. *Cell Stem Cell* 2008 Feb 7;2(2):183-189.

903 (56) Zhu X, Williamson PR. Role of laccase in the biology and virulence of *Cryptococcus*  
904 *neoformans*. *FEMS Yeast Res* 2004 Oct;5(1):1-10.

905 (57) Ellett F, Pase L, Hayman JW, Andrianopoulos A, Lieschke GJ. Mpeg1 Promoter  
906 Transgenes Direct Macrophage-Lineage Expression in Zebrafish. *Blood* 2011 Jan  
907 27;117(4):e49-56.

908 (58) Maskrey BH, Bermudez-Fajardo A, Morgan AH, Stewart-Jones E, Dioszeghy V, Taylor  
909 GW, et al. Activated platelets and monocytes generate four hydroxyphosphatidylethanolamines  
910 via lipoxygenase. *J Biol Chem* 2007 Jul 13;282(28):20151-20163.

911

912

## Fig1

**The intracellular proliferation defect of the *C. neoformans* mutant  $\Delta plb1$ , can be reversed with the addition of exogenous prostaglandin  $E_2$ .** J774 murine macrophages were infected with  $\Delta plb1$ , the parental strain H99 or a genetic reconstitute strain  $\Delta plb1:PLB1$ . Infected cells were left untreated or treated with 2 nM  $PGE_2$  or an equivalent solvent (ethanol) control. Mean IPR from 5 biological repeats shown with error bars representing standard deviation. An unpaired two tailed Student's t-test was performed to compare each treatment group. H99 etoh vs H99 2 nM  $PGE_2$  ns  $p = 0.7212$ ,  $\Delta plb1$  etoh vs.  $\Delta plb1$  2 nM  $PGE_2$  \*  $p = 0.0376$ ,  $\Delta plb1:PLB1$  etoh vs.  $\Delta plb1:PLB1$  2 nM  $PGE_2$  ns  $p=0.723$ .

## Fig2

**The prostaglandin  $E_2$  dependent growth defect of  $\Delta plb1$  is also present *in vivo*: A i** H99-GFP infected larvae imaged at 0, 1, 2 and 3 dpi. At least 50 larvae measured per time point across 3 biological repeats. Box and whiskers show median, 5<sup>th</sup> percentile and 95<sup>th</sup> percentile. Unpaired Mann-Whitney U tests used to compare the burden between each strain for every time point, for p values see (Supplementary Fig 1B ii). **B i** – H99-GFP Infected larvae treated with 10  $\mu M$  prostaglandin  $E_2$  or equivalent solvent (DMSO) control. At least 60 larvae measured per treatment group from 3 biological repeats. Box and whiskers show median, 5<sup>th</sup> percentile and 95<sup>th</sup> percentile. Unpaired Mann-Whitney U tests used to compare between treatments DMSO vs. 10  $\mu M$   $PGE_2$  \*  $p = 0.0137$  (threshold for significance 0.017, corrected for multiple comparisons). **C i**, H99-GFP Infected larvae treated with 10  $\mu M$  prostaglandin  $D_2$  or equivalent solvent (DMSO) control. At least 60 larvae measured per treatment group from 4 biological repeats. Box and whiskers show median, 5<sup>th</sup> percentile and 95<sup>th</sup> percentile. Unpaired Mann-Whitney U tests used to compare between treatments DMSO vs. 10  $\mu M$   $PGD_2$ , ns  $p= 0.8$  **D i**  $\Delta plb1$ -GFP infected larvae (500 cell inoculum injected at 2 dpf) imaged at 0, 1, 2 and 3 dpi. N = 3. Box and whiskers show median, 5<sup>th</sup> percentile and 95<sup>th</sup> percentile. At least 87 larvae



measured for each time point from 3 biological repeats. Unpaired Mann-Whitney U tests used to compare the burden between each strain for every time point, for p values see (Supplementary Fig 1 A i + A ii). **E i**  $\Delta plb1$ -GFP Infected larvae treated with 10  $\mu$ M prostaglandin  $E_2$  or equivalent solvent (DMSO) control. At least 35 larvae measured per treatment group from 2 biological repeats. Box and whiskers show median, 5<sup>th</sup> percentile and 95<sup>th</sup> percentile. Unpaired Mann-Whitney U tests used to compare between treatments  $\Delta plb1$ -GFP DMSO vs 10  $\mu$ M PGE<sub>2</sub> \*\*\* p = 0.0001 (threshold for significance 0.017, corrected for multiple comparisons). **F i**  $\Delta plb1$ -GFP Infected larvae treated with 10  $\mu$ M prostaglandin  $D_2$  or equivalent solvent (DMSO) control. At least 45 larvae measured per treatment group from 3 biological repeats. Box and whiskers show median, 5<sup>th</sup> percentile and 95<sup>th</sup> percentile. Unpaired Mann-Whitney U tests used to compare between treatments DMSO vs. 10  $\mu$ M PGD<sub>2</sub>. Ns p = 0.1 **A ii** Representative GFP images (representative = median value) H99-GFP infected larvae, untreated at 0,1,2,3 dpi. **B ii**, **C ii** Representative GFP images (representative = median value) H99-GFP infected larvae, at 2 dpi treated with 10  $\mu$ M PGE<sub>2</sub> (**B ii**) or PGD<sub>2</sub> (**C ii**). **D ii** Representative GFP images (representative = median value)  $\Delta plb1$ -GFP infected larvae, untreated at 0,1,2,3 dpi. **E ii**, **F ii** Representative GFP images (representative = median value)  $\Delta plb1$ -GFP infected larvae, at 2 dpi treated with 10  $\mu$ M PGE<sub>2</sub> (**E ii**) or PGD<sub>2</sub> (**F ii**).

### Fig 3

#### **The observed activity of PGE<sub>2</sub> is due to its dehydrogenated derivative 15-keto-PGE<sub>2</sub>:**

Fungal burden measured at 2 days post infection (2 dpi) by counting GFP positive pixels in each larvae. **A i** H99-GFP Infected larvae treated with 10  $\mu$ M 16,16-dimethyl-prostaglandin  $E_2$  or equivalent solvent (DMSO) control. At least 75 larvae measured per treatment group from 4 biological repeats. Box and whiskers show median, 5<sup>th</sup> percentile and 95<sup>th</sup> percentile. Unpaired Mann-Whitney U test used to compare between treatments, DMSO vs. 10  $\mu$ M 16, 16-dm PGE<sub>2</sub> ns p = 0.9954. **B i** H99-GFP Infected larvae treated with 10  $\mu$ M 15-keto-prostaglandin  $E_2$  or

equivalent solvent (DMSO) control. At least 55 larvae measured per treatment group from 3 biological repeats. Unpaired Mann-Whitney U test used to compare between treatments DMSO vs. 10  $\mu$ M 15-keto-PGE<sub>2</sub> \*\* p = 0.0048 (threshold for significance 0.017, corrected for multiple comparisons). **C i**  $\Delta plb1$ -GFP Infected larvae treated with 10  $\mu$ M 16, 16-dimethyl prostaglandin E<sub>2</sub> or equivalent solvent (DMSO) control. At least 45 larvae per treatment group from 3 biological repeats. Unpaired Mann-Whitney U test used to compare between treatments  $\Delta plb1$ -GFP DMSO vs 10  $\mu$ M 16, 16-dm PGE<sub>2</sub> ns p = 0.98. **D i**  $\Delta plb1$ -GFP Infected larvae treated with 10  $\mu$ M 15-keto-prostaglandin E<sub>2</sub> or equivalent solvent (DMSO) control. At least 35 larvae measured per treatment group from 2 biological repeats. Unpaired Mann-Whitney U test used to compare between treatments DMSO vs 10  $\mu$ M 15-keto-PGE<sub>2</sub> \* p = 0.0119 (threshold for significance 0.017, corrected for multiple comparisons). **A ii, B ii** Representative GFP images (representative = median value) H99-GFP infected larvae, at 2dpi treated with 10  $\mu$ M 16,16-dm-PGE<sub>2</sub> (**A ii**) or 15-keto-PGE<sub>2</sub> (**B ii**). **C ii, D ii** Representative GFP images (representative = median value)  $\Delta plb1$ -GFP infected larvae, at 2dpi treated with 10  $\mu$ M 16,16-dm-PGE<sub>2</sub> (**C ii**) or 15-keto-PGE<sub>2</sub> (**D ii**). **E** H99-GFP infected larvae treated with a combination of 3  $\mu$ M AH6809 and 3  $\mu$ M GW627368X or equivalent solvent (DMSO) control. Box and whiskers show median, 5<sup>th</sup> percentile and 95<sup>th</sup> percentile. At least 64 larvae measured per treatment group from 4 biological repeats. Mann-Whitney U test used to compare between treatments, no significance found.

#### Fig 4

**Host derived prostaglandins are not required for growth of C. neoformans:** **A** Intracellular proliferation quantified from timelapse movies of J774 macrophages infected with H99-GFP or  $\Delta plb1$ -GFP and treated with 1 mM Aspirin – either for 18 hours before infection (pretreatment) or throughout the time course of infection. One-way ANOVA with Tukey post-test performed



990 comparing all conditions. H99-GFP DMSO vs.  $\Delta plb1$ -GFP DMSO \*\*\*  $p = 0.0002$ . H99-GFP  
991 DMSO vs.  $\Delta plb1$ -GFP 1 mM (pretreat) \*\*\*\*  $p = <0.0001$ . H99-GFP DMSO vs.  $\Delta plb1$ -GFP 1 mM  
992 aspirin \*\*\*  $p = 0.0001$ . H99-GFP + 1mM aspirin (pretreat) vs.  $\Delta plb1$ -GFP DMSO \*\*\*\*  $p <0.0001$ .  
993 H99-GFP + 1mM aspirin (pretreat) vs.  $\Delta plb1$ -GFP 1 mM aspirin (pretreat) \*\*\*\*  $p < 0.0001$ . H99-  
994 GFP + 1mM aspirin (pretreat) vs.  $\Delta plb1$ -GFP 1 mM aspirin \*\*\*\*  $p <0.0001$ . H99-GFP+ 1mM  
995 aspirin vs.  $\Delta plb1$ -GFP DMSO \*\*\*  $p = 0.0001$ . H99-GFP + 1mM aspirin vs.  $\Delta plb1$ -GFP 1 mM  
996 aspirin (pretreat) \*\*\*\*  $p <0.0001$ . H99-GFP+ 1mM aspirin vs.  $\Delta plb1$ -GFP 1 mM aspirin \*\*\*\*  $p <$   
997  $0.0001$ . **B i** H99-GFP infected larvae treated with 15  $\mu$ M NS-398, 15  $\mu$ M SC-560 or equivalent  
998 solvent (DMSO) control. Box and whiskers show median, 5<sup>th</sup> percentile and 95<sup>th</sup> percentile. At  
999 least 25 larvae measured per treatment group from 2 biological repeats. Mann-Whitney U test  
1000 used to compare between treatments, DMSO vs. 15  $\mu$ M \*\*\*  $p = 0.0002$ . **B ii**  $\Delta plb1$ -GFP infected  
1001 larvae treated with 15  $\mu$ M NS-398, 15  $\mu$ M SC-560 or equivalent solvent (DMSO) control. Box  
1002 and whiskers show median, 5<sup>th</sup> percentile and 95<sup>th</sup> percentile. At least 34 larvae measured per  
1003 treatment group from 2 biological repeats. Mann-Whitney U test used to compare between  
1004 treatments, no significance found. **C** 2 dpi zebrafish larvae crispants with CRISPR knockout  
1005 against Prostaglandin E<sub>2</sub> synthase (*ptges*) or a Tyrosinase control (*tyr*) infected with H99-GFP or  
1006  $\Delta plb1$ -GFP, fungal burden quantified at 0 dpi (**C i**) and 3 dpi (**C ii**) – data shown is a single  
1007 experiment but is representative of N=3 experiments. One way ANOVA with Tukey post-test  
1008 performed to compare each condition **C i** no significance found **C ii** H99-GFP + *tyr*<sup>-/-</sup> vs. H99-  
1009 GFP + *ptges*<sup>-/-</sup> \*  $p = 0.0390$ . H99-GFP + *ptges*<sup>-/-</sup> vs.  $\Delta plb1$ -GFP + *tyr*<sup>-/-</sup> \*  $p = 0.0313$ . H99-GFP  
1010 + *ptges*<sup>-/-</sup> vs.  $\Delta plb1$ -GFP + *ptges*<sup>-/-</sup> \*  $p = 0.0121$ . **D i** PGE<sub>2</sub> monoclonal EIA ELISA performed on  
1011 supernatants from *C. neoformans* infected macrophages collected at 18 hr post infection. Mean  
1012 concentration of PGE<sub>2</sub> (pg per 1x10<sup>6</sup> cells) plotted with SD, n = 4. One-way ANOVA with Tukey  
1013 post-test performed, no significance found. **D ii** LC MS/MS mass spectrometry analysis  
1014 performed on cell suspensions (infected J774 cells and supernatants) collected at 18 hr post  
1015 infection. Mean concentration of PGE<sub>2</sub> (pg per 1x10<sup>6</sup> cells) plotted with SD, n = 3. One-way

ANOVA with Tukey post-test performed, no significance found. **E** J774 cells co-infected with a 50:50 mix of  $\Delta plb1$  and H99-GFP. **i** Diagrammatic representation of co-infection experiment. GFP<sup>+</sup> (green) and GFP<sup>-</sup> (yellow) *C. neoformans* cells within the phagosome were quantified at 0 hr, macrophages with a burden ratio of 1:2 or 2:1 were re-analysed at 18 hr, the IPR for  $\Delta plb1$  within 2:1 and 1:2 co-infected cells were calculated by dividing the burden at 18hr by burden at 0 hr for GFP<sup>+</sup> (green) or GFP<sup>-</sup> (yellow) cells. **ii** Quantification of IPR for  $\Delta plb1$  cells within  $\Delta plb1$ :H99-GFP 2:1 or 1:2 co-infected macrophages. At least 35 co-infected macrophages were analysed for each condition over 4 experimental repeats. Student's T test performed to compare ratios – 2:1 vs 1:2 \* p = 0.0137.

# **Fig 5 15-keto-PGE<sub>2</sub> promotes fungal burden by activating host PPAR- $\gamma$ .**

**A i** J774 macrophages treated with Troglitazone (TLT - 0.25  $\mu$ M), an equivalent DMSO control or infected with H99 or  $\Delta plb1$  fixed and stained at 18 hpi with Hoechst and antibody against PPAR- $\gamma$ . Nuclear localization of PPAR- $\gamma$  quantified by measuring nuclear grey value of at least 30 cells per condition. A single experiment is shown that is representative of n = 2. One way ANOVA with Tukey post-test used to compare all conditions. DMSO vs. TLT \*\* p = 0.0049. DMSO vs H99 \*\* p = 0.0040. TLT vs  $\Delta plb1$  \* p = 0.0212. H99 vs.  $\Delta plb1$  \* p = 0.0187. **A ii** Transgenic zebrafish larvae with a GFP PPAR-  $\gamma$  reporter treated with DMSO, 250 nM Troglitazone or 10  $\mu$ M 15-keto-PGE<sub>2</sub> + 250 nM Troglitazone overnight and imaged. Lateral views of 2 dpf embryos, anterior to the left, are shown. **B** J774 murine macrophages infected with  $\Delta plb1$  or the parental strain H99. Infected cells treated with 25  $\mu$ M GW9662 (a PPAR- $\gamma$  antagonist) or equivalent solvent (DMSO) control. Mean IPR from 6 biological repeats shown with error bars representing standard deviation. An unpaired two tailed Student's t-test was performed to compare each treatment group. H99 DMSO vs. H99 25  $\mu$ M GW9662 \* p = 0.026.

1040 **C**  $\Delta plb1$ -GFP infected larvae treated with 10  $\mu$ M 15-keto-PGE<sub>2</sub>, 500 nM GW9662, 10  $\mu$ M 15-  
1041 keto-PGE<sub>2</sub> + 500 nM GW9662 or an equivalent solvent (DMSO) control. Box and whiskers show  
1042 median, 5<sup>th</sup> percentile and 95<sup>th</sup> percentile. At least 35 larvae measured per treatment group from  
1043 2 biological repeats. Mann-Whitney U test used to compare between treatments. DMSO vs. 15-  
1044 keto-PGE<sub>2</sub> \*\*\*\* p < 0.0001 (threshold for significance 0.025, corrected for multiple comparisons),  
1045 15-keto-PGE<sub>2</sub> vs. 15-keto-PGE<sub>2</sub> + 500 nM GW9662 \*\* p = 0.005 (threshold for significance  
1046 0.025, corrected for multiple comparisons) **D-F** 2 day old (2 dpf) *Nacre* zebrafish larvae injected  
1047 with 500 cell inoculum. Fungal burden measured at 2 days post infection (2 dpi) by counting  
1048 GFP positive pixels within each larvae. **D i** H99-GFP Infected larvae treated with 0.55  $\mu$ M  
1049 Troglitazone (TLT) equivalent solvent (DMSO) control. Box and whiskers show median, 5<sup>th</sup>  
1050 percentile and 95<sup>th</sup> percentile. At least 55 larvae measured per treatment group over 3 biological  
1051 repeats. Mann-Whitney U test used to compare between treatments, DMSO vs. 0.55  $\mu$ M  
1052 Troglitazone \*\* p = 0.0044 (threshold for significance 0.025, corrected for multiple comparisons).  
1053 **E i**  $\Delta plb1$ -GFP infected larvae treated with 0.55  $\mu$ M Troglitazone (TLT) equivalent solvent  
1054 (DMSO) control. Box and whiskers show median, 5<sup>th</sup> percentile and 95<sup>th</sup> percentile. At least 35  
1055 larvae measured per treatment group from 2 biological repeats. Mann-Whitney U test used to  
1056 compare between treatments, DMSO vs. 0.55  $\mu$ M Troglitazone \*\* p = 0.0089 (threshold for  
1057 significance 0.025, corrected for multiple comparisons). **F i**  $\Delta lac1$ -GFP infected larvae treated  
1058 with 0.55  $\mu$ M Troglitazone (TLT) equivalent solvent (DMSO) control. At least 60 larvae  
1059 measured per treatment group from 3 biological repeats. Box and whiskers show median, 5<sup>th</sup>  
1060 percentile and 95<sup>th</sup> percentile, DMSO vs. 0.55  $\mu$ M Troglitazone \* p = 0.01 (threshold for  
1061 significance 0.025, corrected for multiple comparisons). **D ii, E ii and F ii**, Representative GFP  
1062 images (representative = median value) *C. neoformans* infected larvae, at 2 dpi treated with  
1063 0.55  $\mu$ M Troglitazone (TLT) **D ii** - H99-GFP, **E ii** -  $\Delta plb1$ -GFP and **F ii**  $\Delta lac1$ -GFP.

1064 **Supplementary Fig 1**

**A** Quantification of the viability of *C. neoformans* retrieved from the phagosomes of J774 macrophages at 2 hr and 20 hr post infection. Prior to, and during infection J774 macrophages were treated with 2 mM PGE<sub>2</sub> or the equivalent amount of solvent (Ethanol) *Cryptococcus* cells were counted with a hemocytometer / diluted and plated to give an expected number of 200 CFU - dead *Cryptococcus* cells are indistinguishable from live cells when counting with a hemocytometer however a lower than expected CFU count would indicate that there is a decrease in viability. Data is displayed as the fold change between the CFU count at 2 hpi and 20 hpi for each condition. A one-way ANOVA with Tukey post test was performed comparing all conditions. H99 ETOH vs.  $\Delta plb1$  \*\*  $p = 0.0052$ , H99 ETOH vs.  $\Delta plb1$  ETOH \*\*  $p = 0.0056$ , H99 ETOH vs.  $\Delta plb1$  2 mM PGE<sub>2</sub> \*  $p = 0.029$ . **B i** Comparison of fungal burden between H99-GFP,  $\Delta plb1$ -GFP and  $\Delta lac1$ -GFP infected larvae (Data reproduced from Fig2 Ai, Di and Supplementary Fig 2 Bi for clarity) H99-GFP,  $\Delta plb1$ -GFP and  $\Delta lac1$ -GFP infected larvae imaged at 0, 1, 2 and 3 dpi. At least 50 larvae measured per time point from 3 biological repeats. Box and whiskers show median, 5<sup>th</sup> percentile and 95<sup>th</sup> percentile. Unpaired Mann-Whitney U tests used to compare the burden between each strain for every time point. **B ii** Table of Mann-Whitney U tests comparing burden for each strain between time points. **C** Whole body macrophage counts of zebrafish larvae treated at 2 dpf with 10  $\mu$ M PGE<sub>2</sub>, 10  $\mu$ M 15-keto-PGE<sub>2</sub> or an equivalent DMSO control for 2 days. Box and whiskers show median, 5<sup>th</sup> percentile and 95<sup>th</sup> percentile. At least 12 larvae quantified per treatment group per biological repeat  $n = 4$ . Mann-Whitney U test used to treatments to DMSO control \*\*  $p = 0.0025$ .

## Supplementary Fig 2

**A** J774 cells co-infected with a 50:50 mix of  $\Delta lac1$ -GFP and H99. Quantification of IPR for  $\Delta lac1$ -GFP cells within  $\Delta lac1$ -GFP:H99 2:1 or 1:2 co-infected macrophages. At least 20 co-infected macrophages were analysed for each condition over 4 experimental repeats. Student's T test performed to compare ratios – 2:1 vs 1:2 \*  $p = 0.012$ . **B i**  $\Delta lac1$ -GFP infected larvae

imaged at 0, 1, 2 and 3 dpi. Fungal burden measured by counting GFP positive pixels in each larvae. At least 78 larvae measured per time point across 3 biological repeats. Box and whiskers show median, 5<sup>th</sup> percentile and 95<sup>th</sup> percentile. Unpaired Mann-Whitney U tests used to compare the burden between each strain for every time point, for p values see (Supplementary Fig2 A + B). **B ii** Representative GFP images (representative = median value) of 2dpi  $\Delta lac1$ -GFP infected larvae, untreated at 0,1,2,3 dpi **C i**  $\Delta lac1$ -GFP Infected larvae treated with 10  $\mu$ M prostaglandin E<sub>2</sub> or equivalent solvent (DMSO) control. At least 70 larvae measured per treatment group across 4 biological repeats. Box and whiskers show median, 5<sup>th</sup> percentile and 95<sup>th</sup> percentile. Unpaired Mann-Whitney U test used to compare between treatments, DMSO vs. 10  $\mu$ M PGE<sub>2</sub> \* p = 0.035. **D i**  $\Delta lac1$ -GFP Infected larvae treated with 10  $\mu$ M 16,16-dimethyl prostaglandin E<sub>2</sub> or equivalent solvent (DMSO) control. At least 75 larvae measured per treatment group across 4 biological repeats. Box and whiskers show median, 5<sup>th</sup> percentile and 95<sup>th</sup> percentile. Unpaired Mann-Whitney U test used to compare between treatments, DMSO vs. 10  $\mu$ M 16,16-dimethyl prostaglandin E<sub>2</sub> ns p = 0.062. **E i**  $\Delta lac1$ -GFP Infected larvae treated with 10  $\mu$ M 15-keto-prostaglandin E<sub>2</sub> or equivalent solvent (DMSO) control. At least 58 larvae measured per treatment group across 3 biological repeats. Unpaired Mann-Whitney U test used to compare between treatments DMSO vs. 10  $\mu$ M 15-keto-prostaglandin E<sub>2</sub> ns p= 0.50. **C ii, D ii, E ii** Representative GFP images (representative = median value)  $\Delta lac1$ -GFP infected larvae, at 2 dpi treated with 10  $\mu$ M PGE<sub>2</sub> (**C ii**), 16,16-dm-PGE<sub>2</sub> (**D ii**) or 15-keto-PGE<sub>2</sub> (**E ii**).

### Supplementary Fig 3

**A** PGE<sub>2</sub> monoclonal EIA ELISA performed on supernatants from *C. neoformans* infected macrophages collected at 18 hr post infection. Mean concentration of PGE<sub>2</sub> (pg per 1x10<sup>6</sup> cells) plotted with SD, n = 2. **B** Quantification of IPR for  $\Delta plb1$  cells within  $\Delta plb1$ :H99-GFP co-infected

macrophages at initial burdens of 2:1, 3:1, 4:1 and vice versa. N=4. Student's T test performed to compare ratios – 2:1 vs 1:2 \* p = 0.0137. **C** Example images of immunofluorescence experiments in J774 macrophages staining for PPAR-gamma nuclear localization (for quantification see Fig 5 Ai). J774 cells treated with DMSO, 0.25  $\mu$ M Troglitazone, infected with H99-GFP or  $\Delta plb1$ -GFP at x60 magnification, scale bar = 10  $\mu$ M. Images provided are from the Cy3 channel (PPAR-  $\gamma$ ) and the corresponding cell in DIC. The area of the nuclei is marked with a white dotted line.

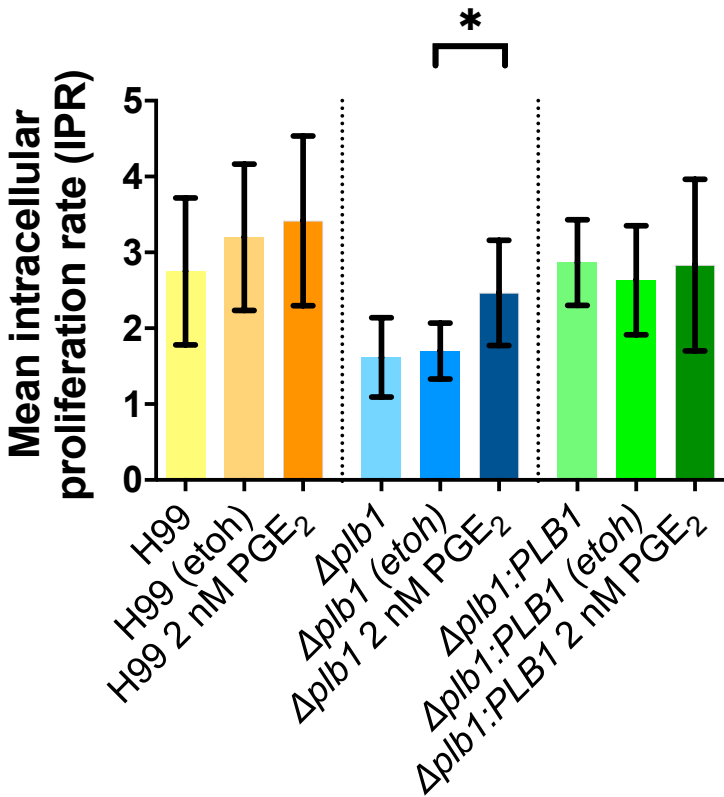
# **Supplementary Fig 4**

Genotyping to confirm zebrafish *ptges* CRISPR. Zebrafish were genotyped post assay (5 dpf), an area of genomic DNA spanning the *ptges* gene ATG site (the CRISPR target) was amplified with PCR to produce a 345 bp product. This product was digested with MwoI to produce genotype specific banding patterns **A**. Schematic of the banding patterns expected for each genotype following MwoI digestion – 1. Undigested product, a single 345 bp band 2. Wild type genotype, 184, 109 and 52 bp bands 3. Hetrozygous genotype (*ptges*<sup>+/−</sup>) 293, 184, 109 and 52 bp bands 4. Homozygous genotype (*ptges*<sup>−/−</sup>) strong bands for 293 and 52 bp, weaker bands at 184 and 109 bp can sometimes be seen indicating a small amount of wildtype *ptges* is still present (this is thought to be beneficial as low levels of *ptges* are required for larvae survival. **B** Genotyping for H99 infected larvae, L = DNA ladder (NEB 50 bp ladder), wt = undigested wild type control, wt dig = wild type digested control, numbers correspond to individual larvae genotyped. H99 + tyro = *tyr*<sup>−/−</sup> larvae infected with H99-GFP. H99 + *ptges* = *ptges*<sup>−/−</sup> larvae infected with H99-GFP **C** Genotyping for  $\Delta plb1$  infected larvae , L = DNA ladder (NEB 50 bp ladder), wt = undigested wild type control, wt dig = wild type digested control, numbers correspond to individual larvae genotyped.  $\Delta plb1$ + tyro = *tyr*<sup>−/−</sup> larvae infected with  $\Delta plb1$ -GFP.  $\Delta plb1$ + *ptges* = *ptges*<sup>−/−</sup> larvae infected with  $\Delta plb1$ -GFP.


1141

1142

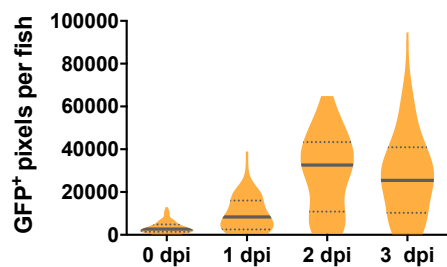
1143



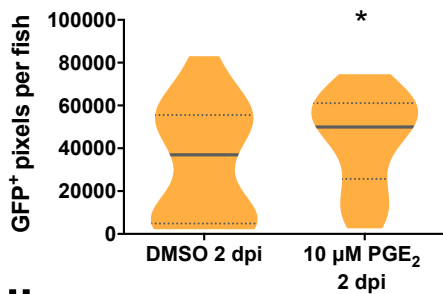


 H99-GFP

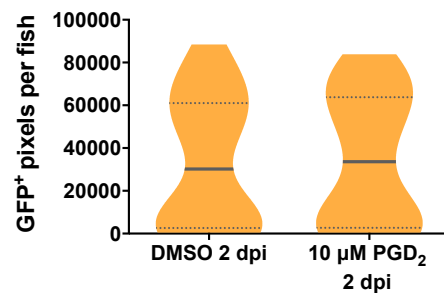
**A i**



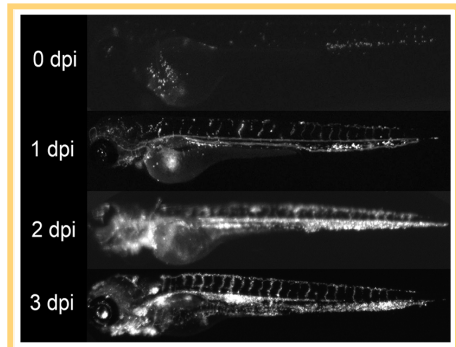
**B i**



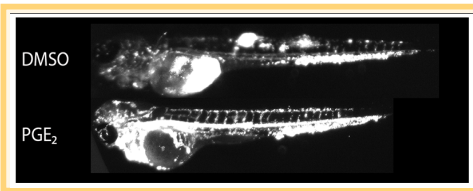
**C i**



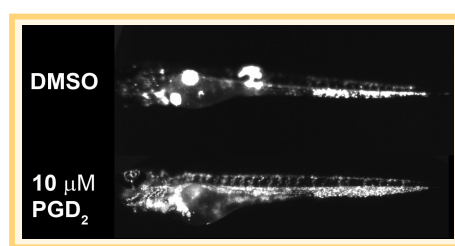
**ii**




**ii**

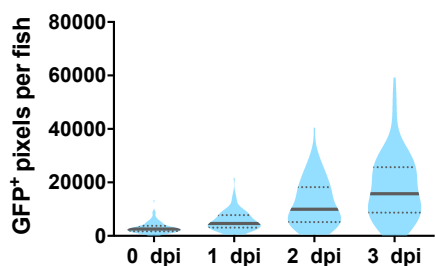


**ii**

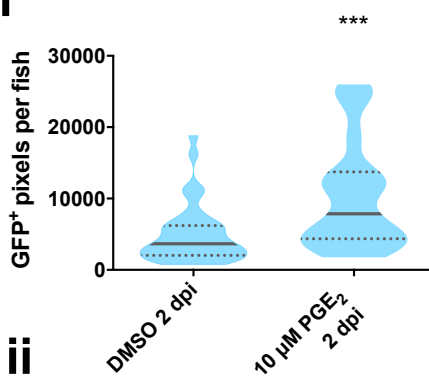


  $\Delta plb1$ -GFP

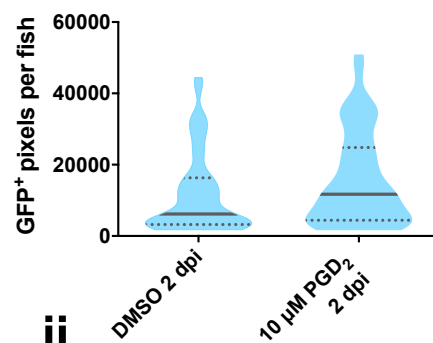
**D i**



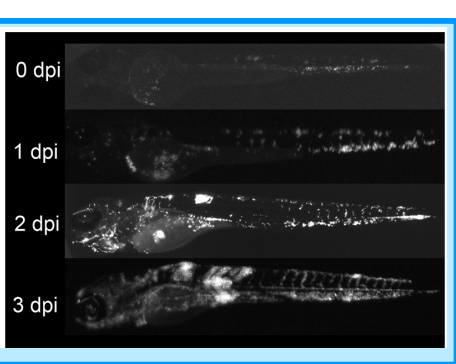
**E i**



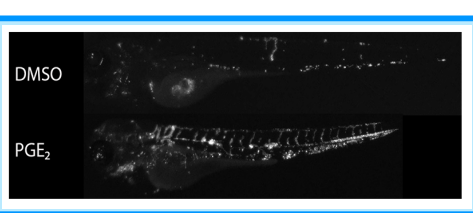
**F i**



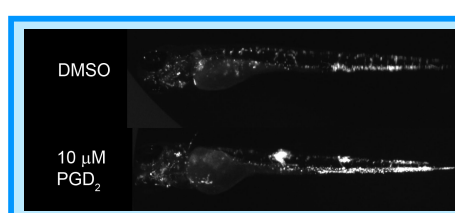
**ii**




**ii**

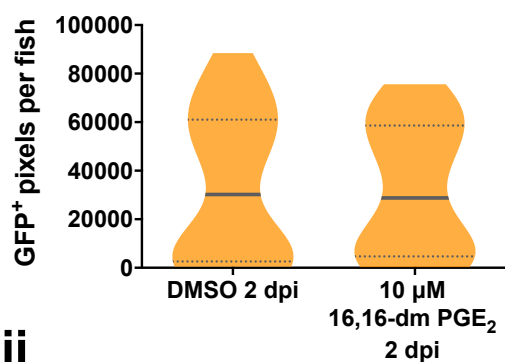


**ii**

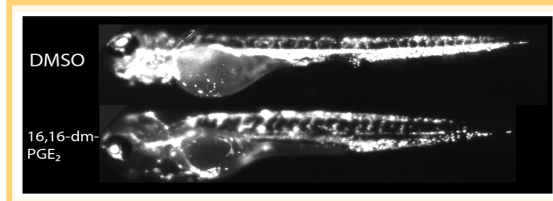


 H99-GFP

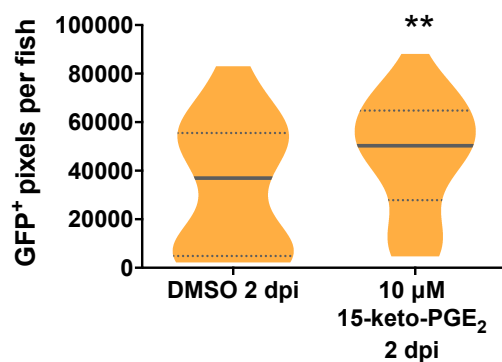
**A i**



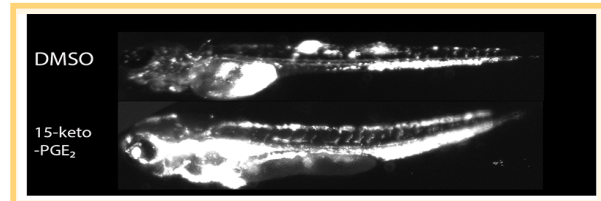
**ii**




**B i**

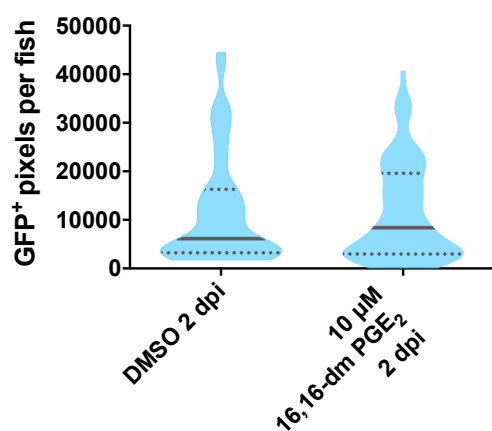


**ii**

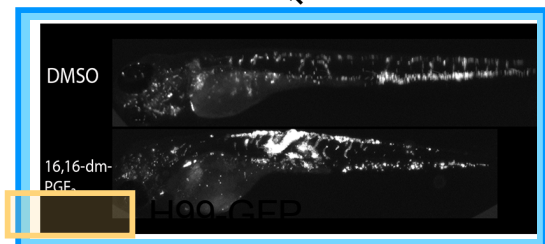


  $\Delta plb1$ -GFP

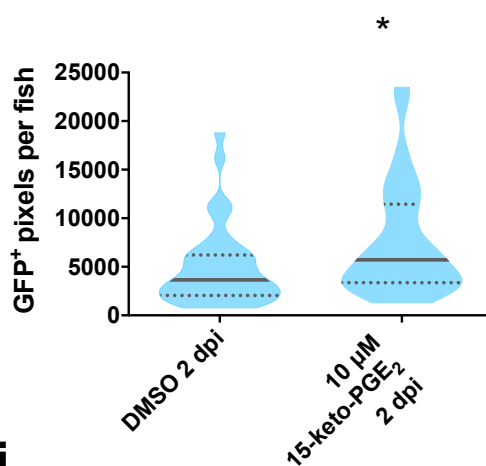
**C i**



**ii**



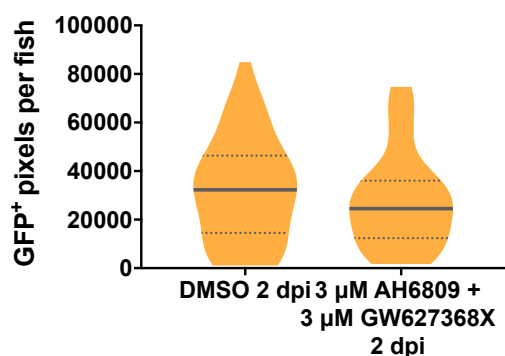
**D i**

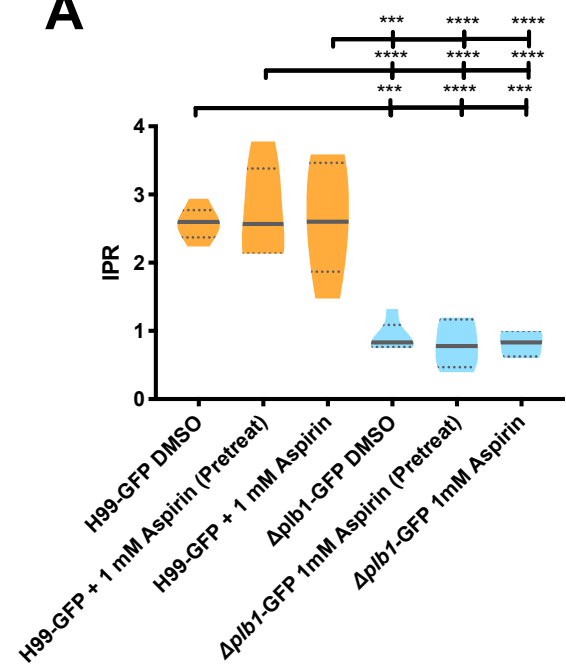
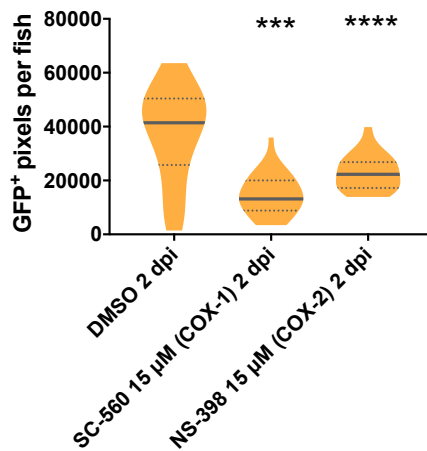
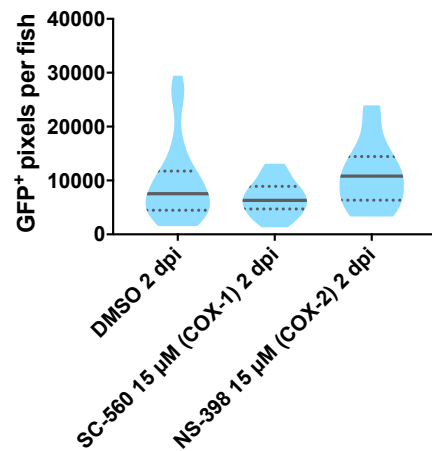
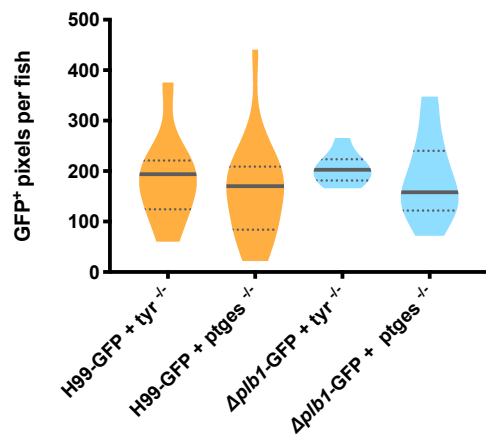
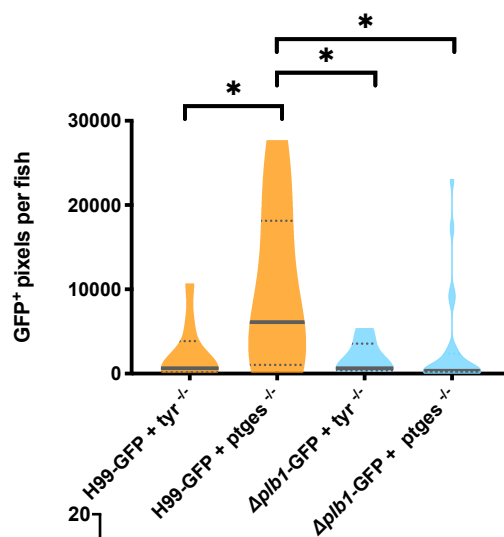
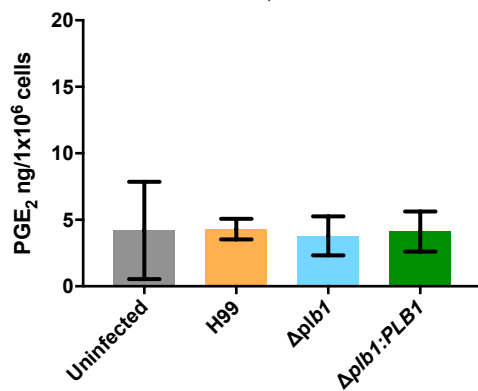
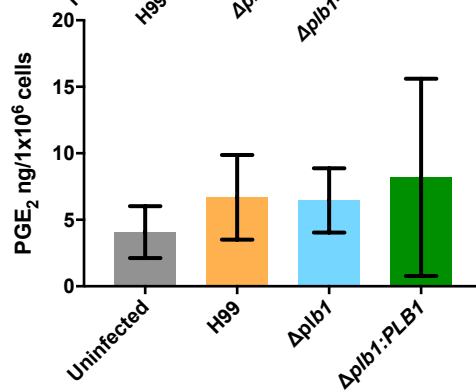
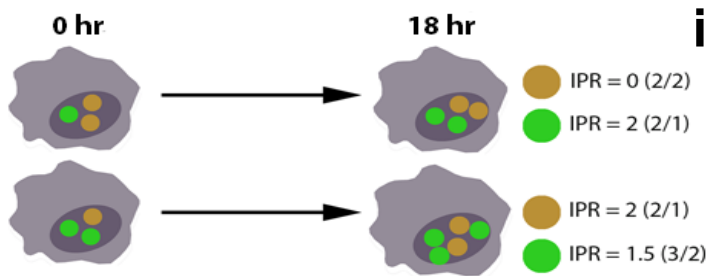
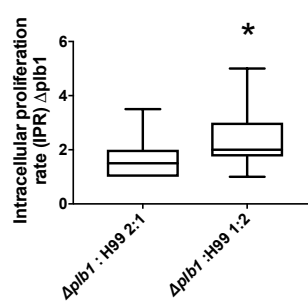


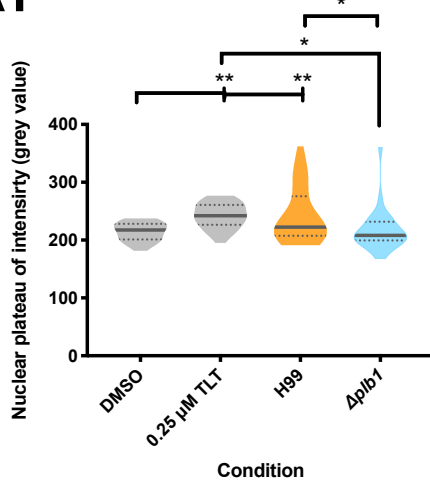
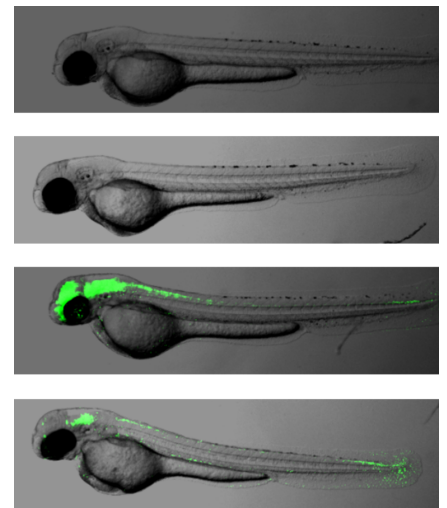
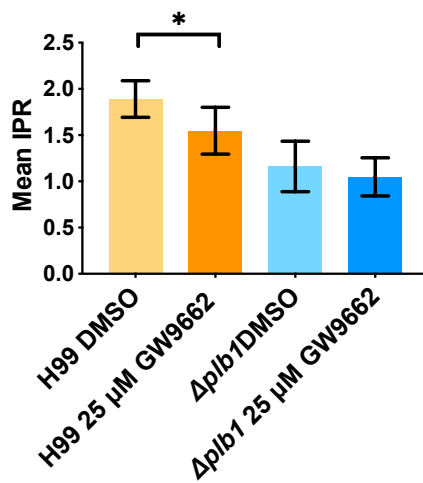
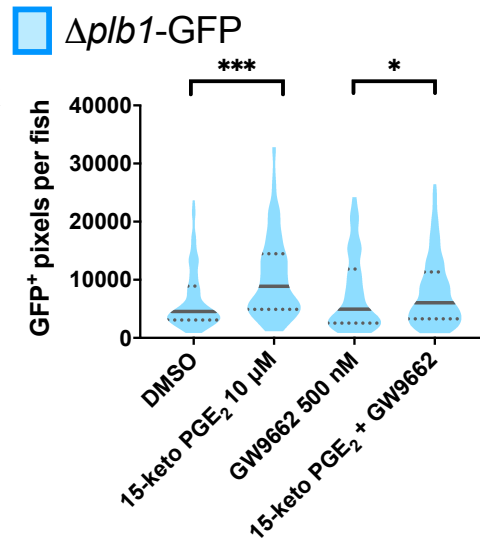
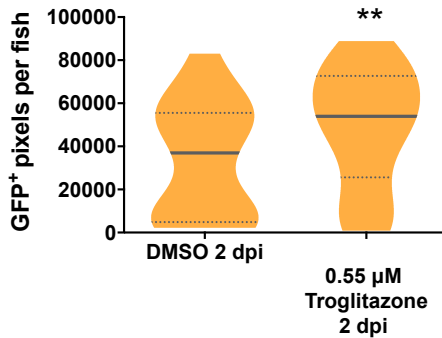
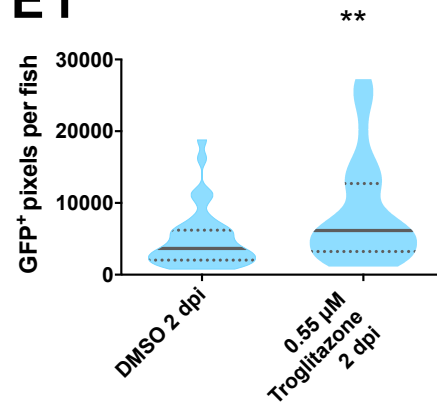
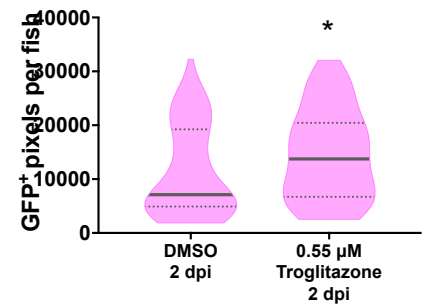
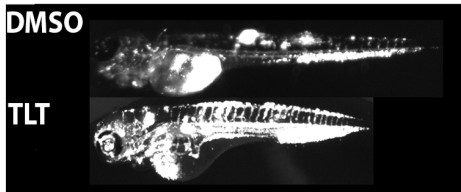
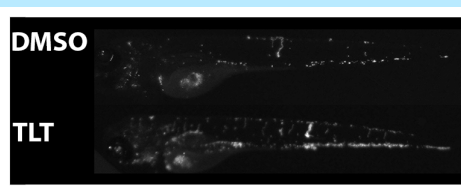
**ii**



**E**



**A****B i****ii****C i****ii****D i****ii****E i****ii**

**Ai****ii****DMSO****10  $\mu$ M 15-keto PGE<sub>2</sub>****0.25  $\mu$ M TLT****0.25  $\mu$ M TLT +  
10  $\mu$ M 15-keto PGE<sub>2</sub>****B****C****H99-GFP** **$\Delta$ plb1-GFP** **$\Delta$ lac1-GFP****Di****Ei****Fi****ii****ii****ii**